OAK RIDGE
NATIONAL LABORATORY
MANAGED BY UT-BATTELLE
FOR THE DEPARTMENT OF ENERGY

ORNL/TM-2005/541

Results from ORNL Characterization of Nominal 350 µm NUCO Kernels from the BWXT 59344 Batch

John D. Hunn, Andrew K. Kercher,
Paul A. Menchhofer and Jeff R. Price

January 2005

UT-BATTELLE
ORNL-27 (4-00)

ORNL/CF-05/02
Revision 0

Results from ORNL Characterization of Nominal 350 μm NUCO Kernels from the BWXT 59344 batch

J.D. Hunn, Oak Ridge National Laboratory

This document is a compilation of characterization data obtained on nominal 350 μm natural enrichment uranium oxide/uranium carbide kernels (NUCO) produced by BWXT for the Advanced Gas Reactor Fuel Development and Qualification Program. These kernels were produced as part of a development effort at BWXT to address issues involving forming and heat treatment and were shipped to ORNL for additional characterization and for coating tests. The kernels were identified as G73N-NU-59344. 250 grams were shipped to ORNL. Size, shape, and microstructural analysis was performed. These kernels were preceded by G73B-NU-69300 and G73B-NU-69301, which were kernels produced and delivered to ORNL earlier in the development phase. Characterization of the kernels from G73B-NU-69300 was summarized in ORNL/CF-04/07 "Results from ORNL Characterization of Nominal 350 μm NUCO Kernels from the BWXT 69300 composite".

Table of Contents

1 Size and Shape Measurement:

J.D. Hunn, A.K. Kercher, and J.R. Price

A sample was riffled from the 250 g batch of NUCO kernels (batch 59344). Size and shape were measured by shadow imaging with an optical microscope the sample of kernels in a random plane. Image analysis software was used to find the center of each kernel and identify 360 points around the perimeter. Data was extracted as both radius and diameter. The terms “radius” and “diameter” are used loosely. “Radius” means the distance from the fit center to the edge. “Diameter” means the distance from edge to edge in a line passing through the fit center. Data for each kernel was then reported in terms of the mean radius or diameter, the standard deviation in those values, the minimum and maximum radius and diameter, and the ratio of the maximum over the minimum of those values. These values for each kernel were then compiled and the average, standard deviation, minimum, and maximum for each value was calculated. In addition to reporting the compiled data for the sample, histograms of the mean kernel radius or diameter and the aspect ratios have also been provided to show how these values were distributed in the sample analyzed.

Figure 1-1 shows the summary data for the measured radius of 3331 kernel shadowgraphs. Figure 1-2 shows the same data reported in terms of the diameter. The difference between compiling the measurements in terms of radius versus diameter is that the radius based measurements more accurately report non-symmetric shapes. The diameter measurements dilute the effect of a local deviation in radius by adding the opposite radius (+180 degrees in polar coordinates). Because the kernels were nearly spherical, there was no significant difference in the statistically calculated mean diameter from twice the mean radius. Even the standard deviations in these values scale by a factor of two. However, the max/min aspect ratio was significantly affected. This is because these values are based on maximum and minimums as opposed to means. R_{max}/R_{min} is a more sensitive way of measuring the deviation from perfectly spherical. The R_{max}/R_{min} measurement showed a higher average aspect ratio.

The measured mean diameter for this sample was 384 μm with a standard deviation of 8 μm. The 95% confidence interval for the batch was 383-385 μm. The measured aspect ratio (D_{max}/D_{min}) was 1.024 with a standard deviation of 0.014. 2.6% of the sample measured had an aspect ratio above 1.06. Figure 1-3 and Figure 1-4 show how the measured size and shape of batch 59344 compare to the previously analyzed NUCO composite.

	Radius Aspect Ratio	Mean Radius	St. Dev. In Radius	Minimum Radius	Maximum Radius
Average	1.04	192	1.6	188	196
Standard Deviation	0.02	4	0.9	5	5
Minimum	1.01	126	0.4	117	129
Maximum	1.39	212	18	207	230

Aspect Ratio (R)	*Frequency*
1	0
1.01	3
1.02	357
1.03	993
1.04	820
1.05	479
1.06	240
1.07	155
1.08	90
1.09	57
1.1	46
1.11	31
1.12	19
1.13	13
1.14	9
1.15	4
1.16	4
1.17	1
1.18	2
1.19	1
1.2	1
1.21	2
1.22	1
More	3

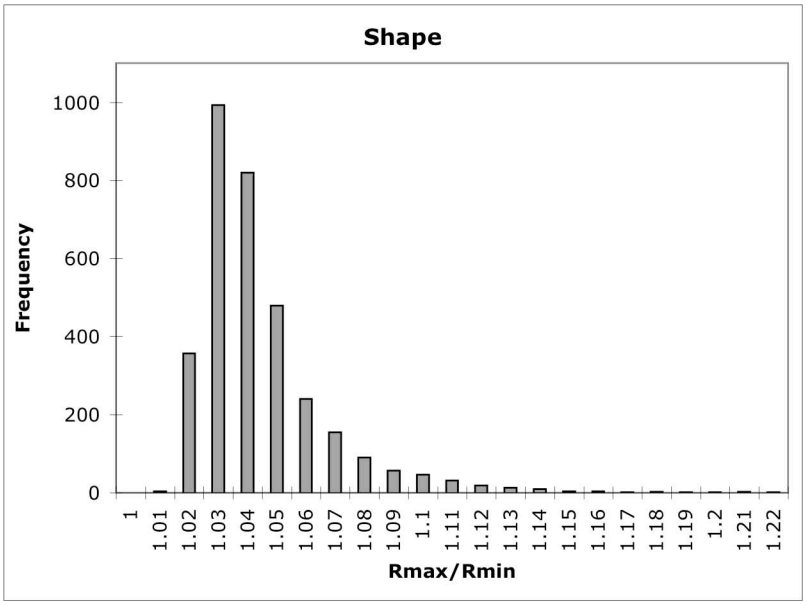

Mean Radius	*Frequency*
Less	7
180	5
182	20
184	66
186	208
188	258
190	331
192	390
194	715
196	1017
198	223
200	59
202	13
204	8
More	11

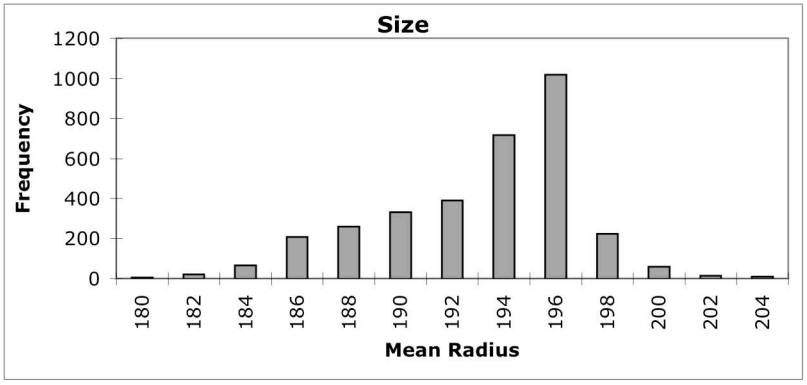

Figure 1-1: Size and shape summary for 3331 NUCO kernels. Measurements are distance from best circle fit center to edge in μm.

	Diameter Aspect Ratio	Mean Diameter	St. Dev. In Diameter	Minimum Diameter	Maximum Diameter
Average	1.024	384	2	380	389
Standard Deviation	0.014	8	1.5	9	9
Minimum	1.004	253	0.5	244	256
Maximum	1.217	425	25	418	447

Aspect Ratio (D)	*Frequency*
1	0
1.005	1
1.01	154
1.015	619
1.02	818
1.025	644
1.03	430
1.035	219
1.04	124
1.045	93
1.05	64
1.055	38
1.06	39
1.065	26
1.07	14
1.075	10
1.08	10
1.085	3
1.09	6
1.095	2
1.1	4
1.105	3
1.11	3
1.115	2
More	5

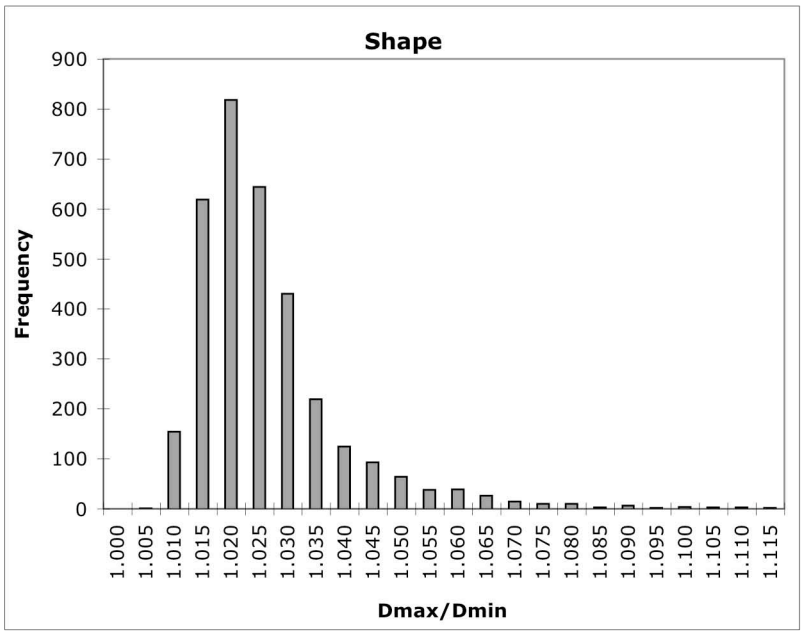

Mean Diameter	*Frequency*
Less	9
362	10
366	38
370	137
374	239
378	289
382	358
386	505
390	1012
394	575
398	104
402	30
406	9
410	7
More	9

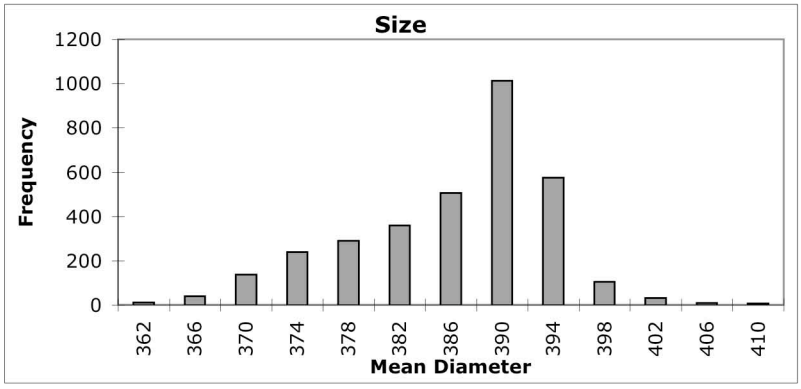

Figure 1-2: Size and shape summary for 3331 NUCO kernels. Measurements are in μm from edge to edge through best circle fit center.

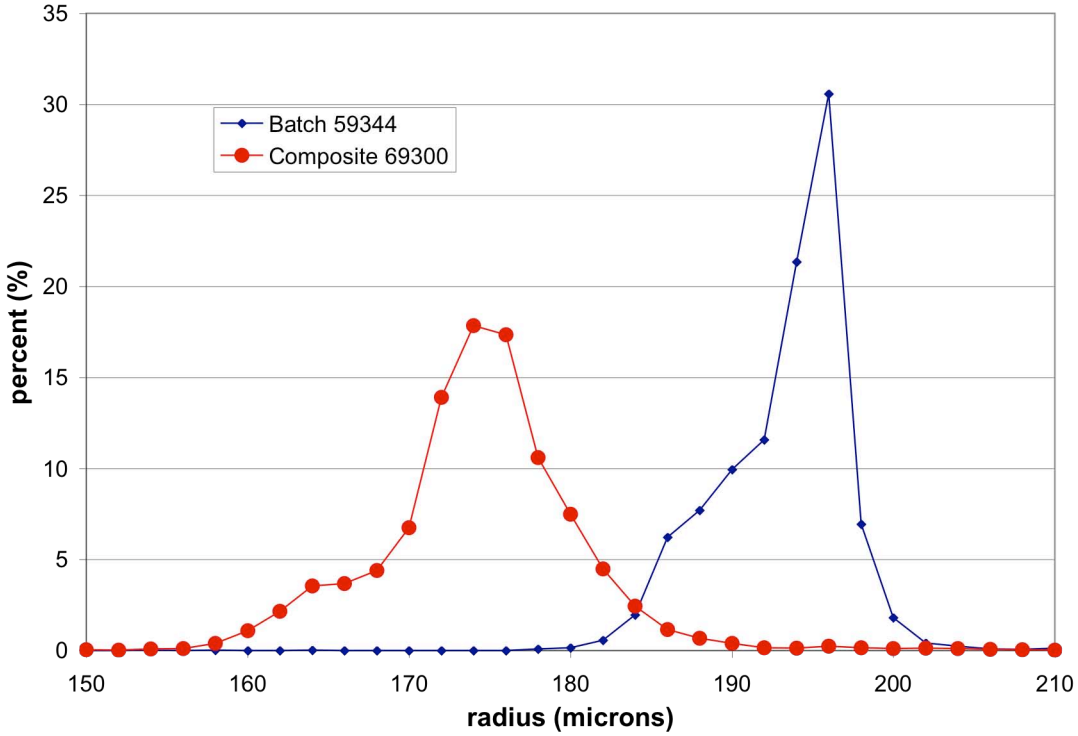

Figure 1-3: Comparison of kernel radius between batch 59344 and composite 69300.

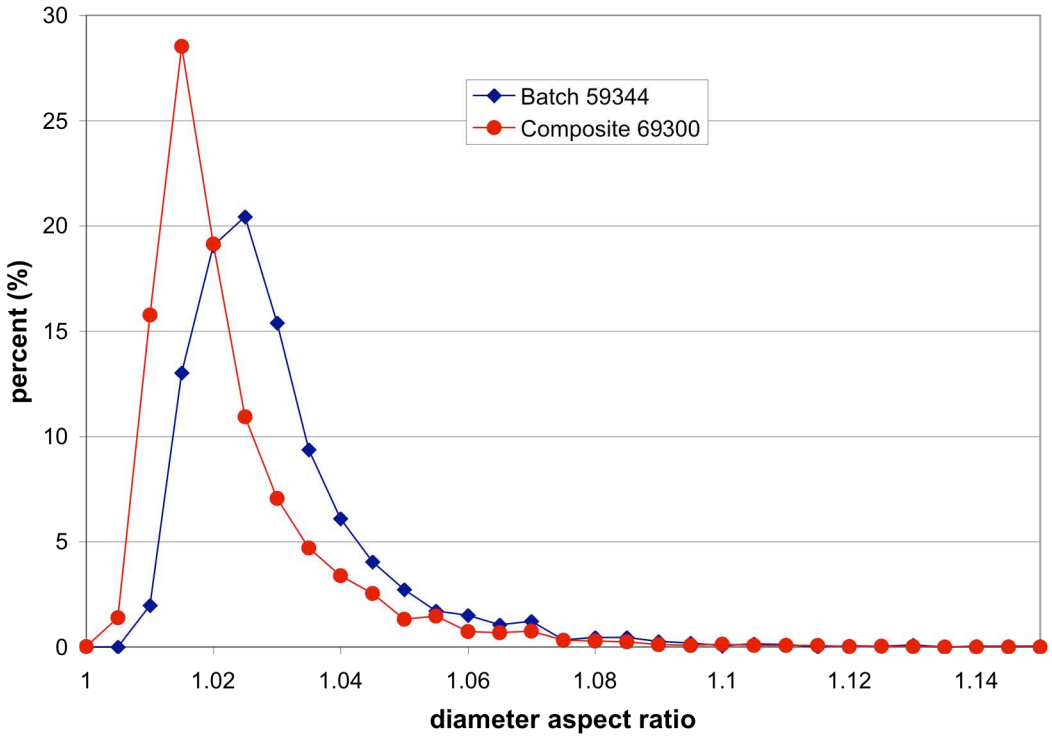

Figure 1-4: Comparison of aspect ratio between batch 59344 and composite 69300.

2 Optical and SEM Analysis of Kernel Surface

J.D. Hunn and P.A. Menchhofer

A sample of the NUCO kernels was observed under the optical stereo microscope (Figure 2-1 through Figure 2-6). Some kernels were relatively smooth and shiny; the microscope's ring light was reflected as a white ring from each kernel. Some kernels were lumpy. This variation in surface structure was observed for the previously reported 69300 composite as well (Figure 2-2 and Figure 2-4). Whereas the previous kernels were from a composite, the kernels currently being analyzed were from a single green kernel batch (29323). The observed variation in surface structure may therefore indicate that there is a non-uniformity during the kernel forming process, perhaps a degradation over time.

A smooth and a lumpy kernel were selected at random and the surface was imaged by Scanning Electron Microscopy (SEM). This was done for quick qualitative analysis and informational purposes and is not expected to be a statistically adequate analysis of the average microstructure of each type. Figure 2-7 through Figure 2-9 show a smooth kernel. These kernels were similar to those categorized as type 1 and type 4 in the previous report (ORNL/CF-04/07). Figure 2-10 through Figure 2-12 show a lumpy kernel. These kernels were similar to the previously categorized type 3 kernels but, in this newer batch, the surfaces were somewhat smoother and the surface grains were larger. A few kernels showed an unusual "crystallized" surface. Examples are shown in Figure 2-6 and Figure 2-13 through Figure 2-15. These kernels typically showed large protruding grains on one half of the kernel and smooth surfaces with large pores on the opposite side.

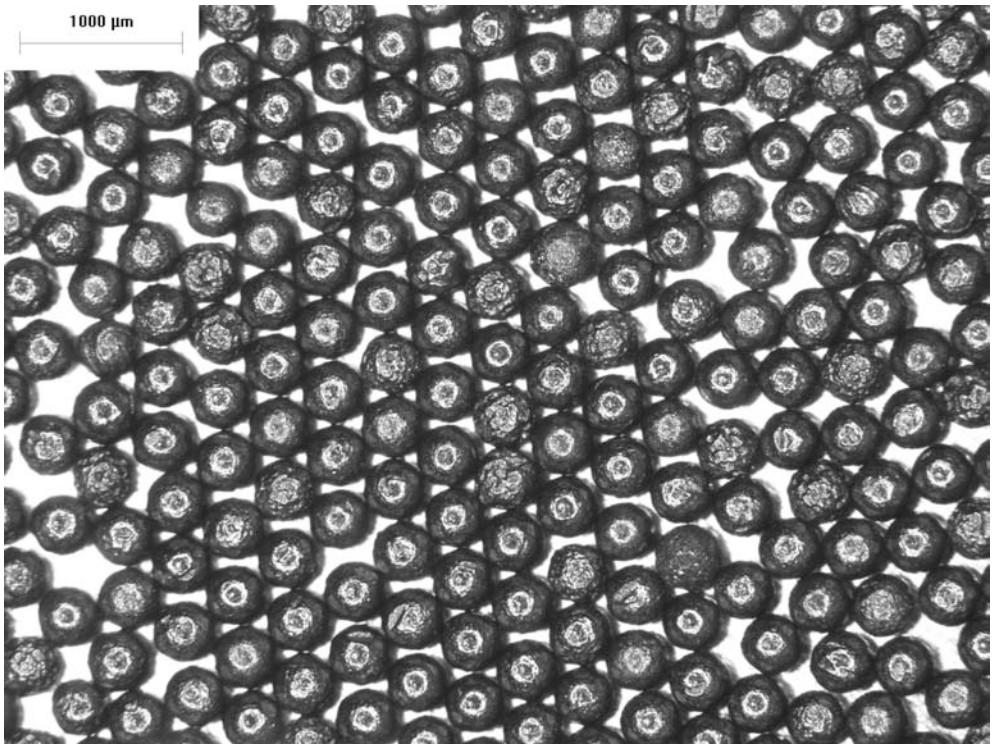

Figure 2-1: Optical image of NUCO kernel batch 59344.

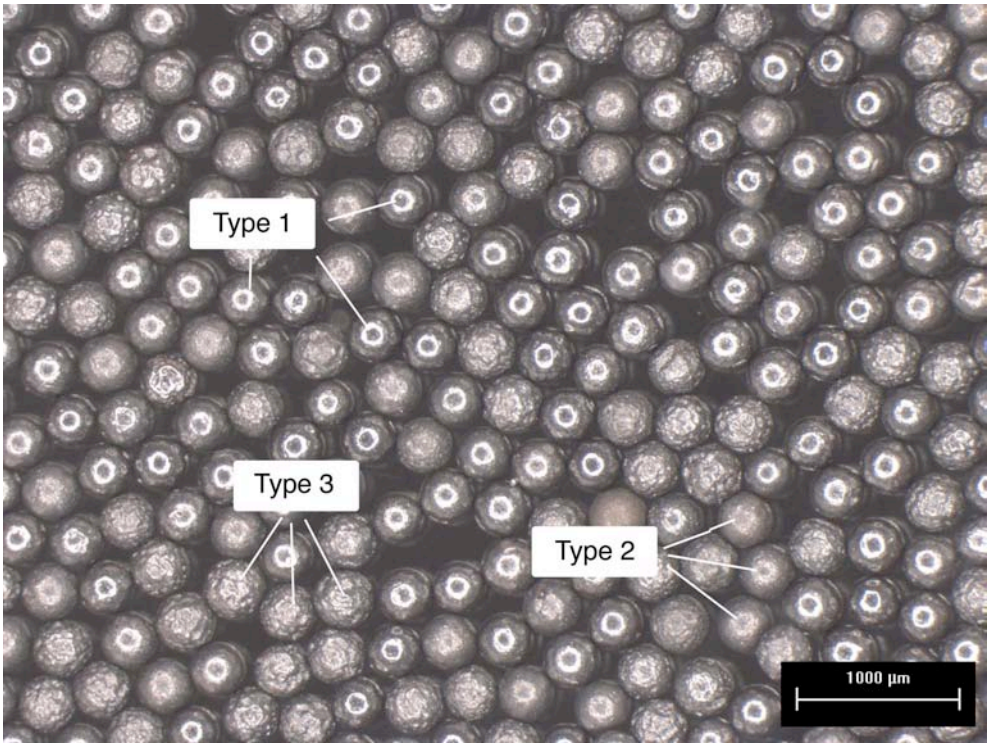

Figure 2-2: Optical image of NUCO kernel composite 69300.

Figure 2-3: Optical image of NUCO kernel batch 59344.

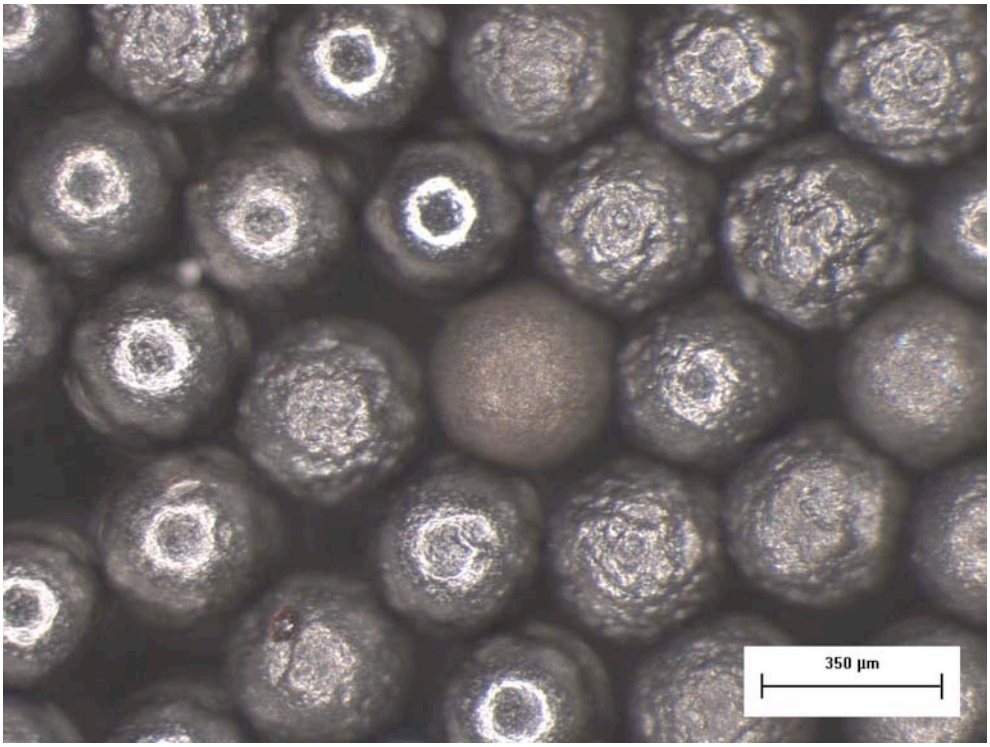

Figure 2-4: Optical image of NUCO kernel composite 69300.

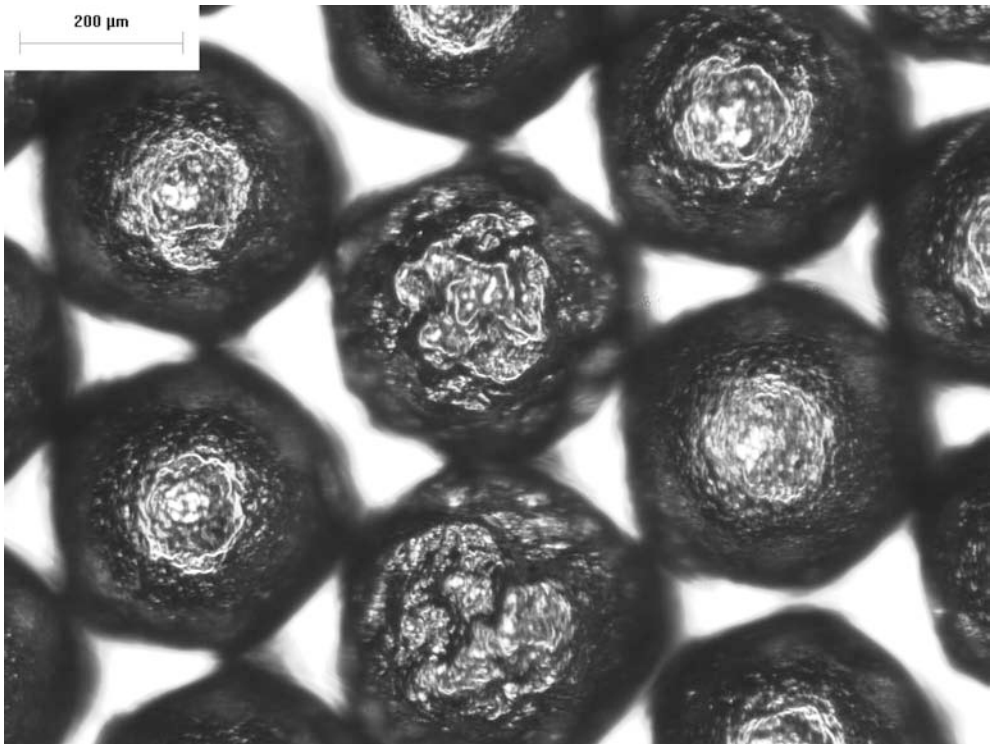

Figure 2-5: Optical image of NUCO kernel batch 59344.

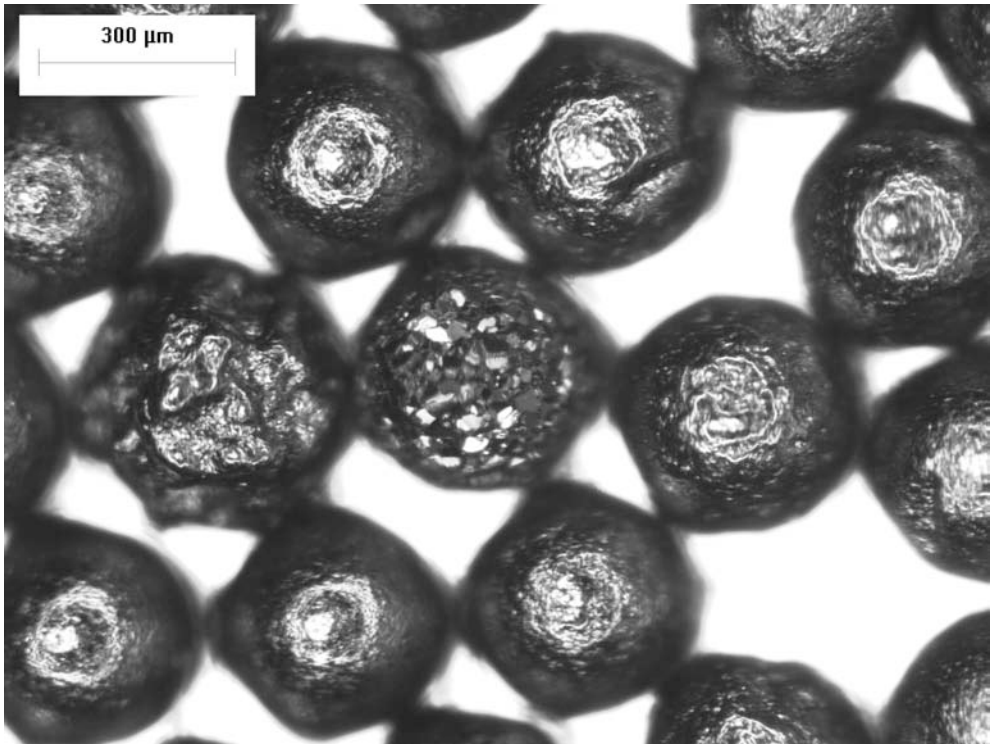

Figure 2-6: Optical image of NUCO kernel batch 59344.

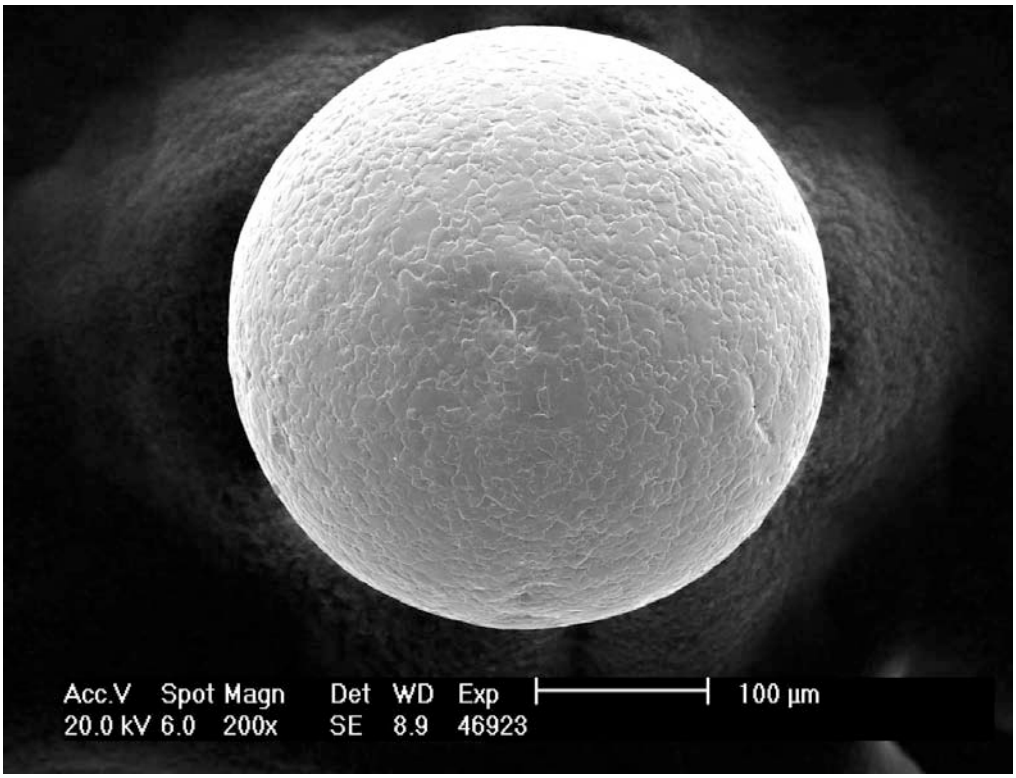

Figure 2-7: Smooth NUCO kernel from 59344 batch.

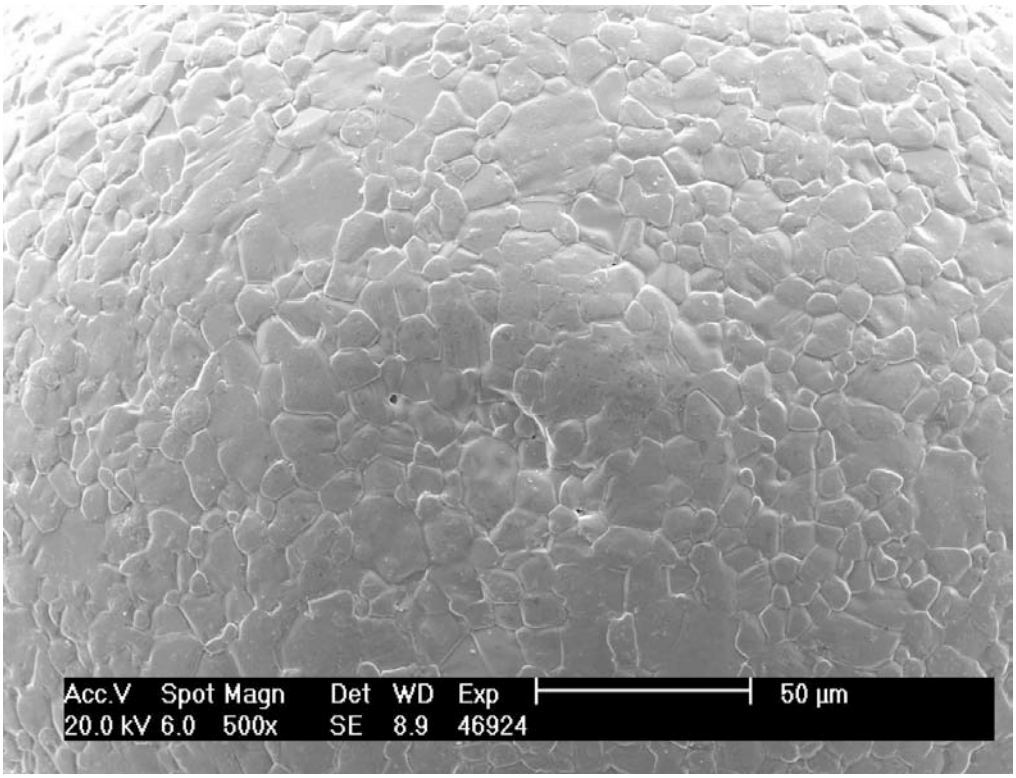

Figure 2-8: Smooth NUCO kernel from 59344 batch.

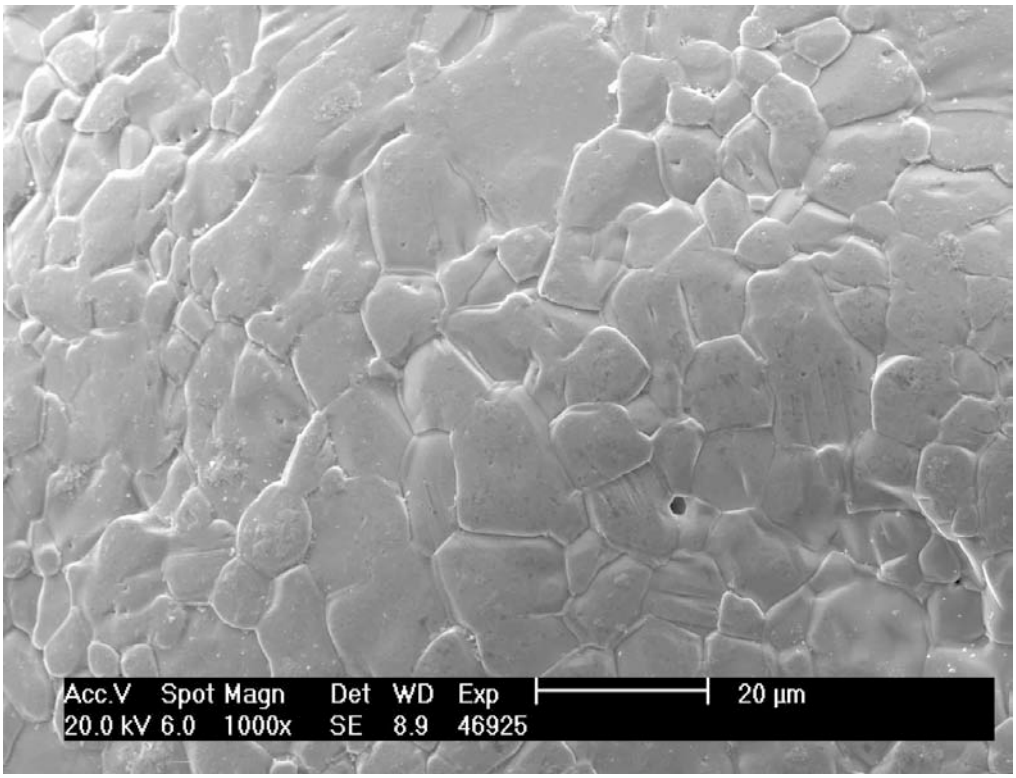

Figure 2-9: Smooth NUCO kernel from 59344 batch.

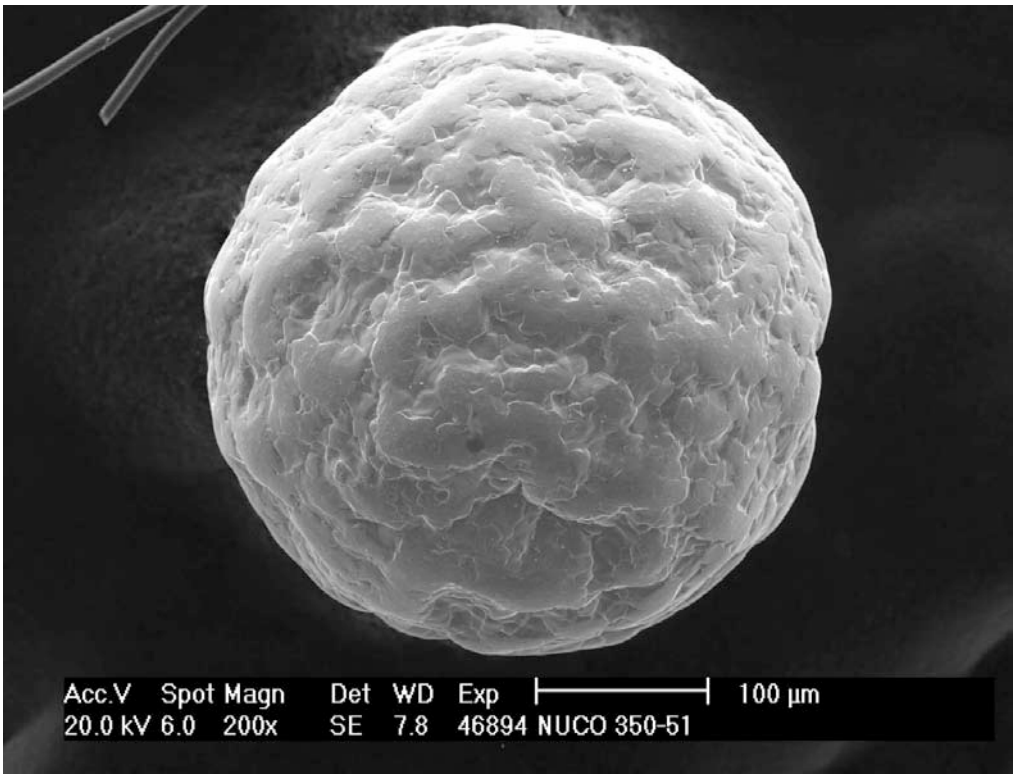

Figure 2-10: Lumpy NUCO kernel from 59344 batch.

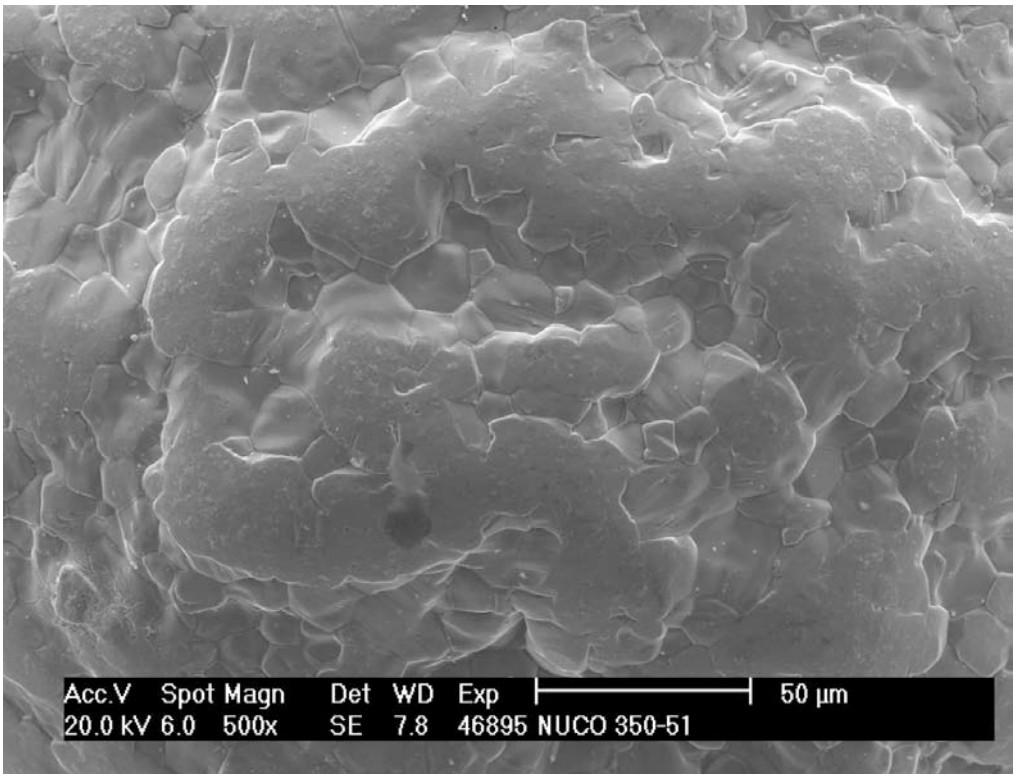

Figure 2-11: Lumpy NUCO kernel from 59344 batch.

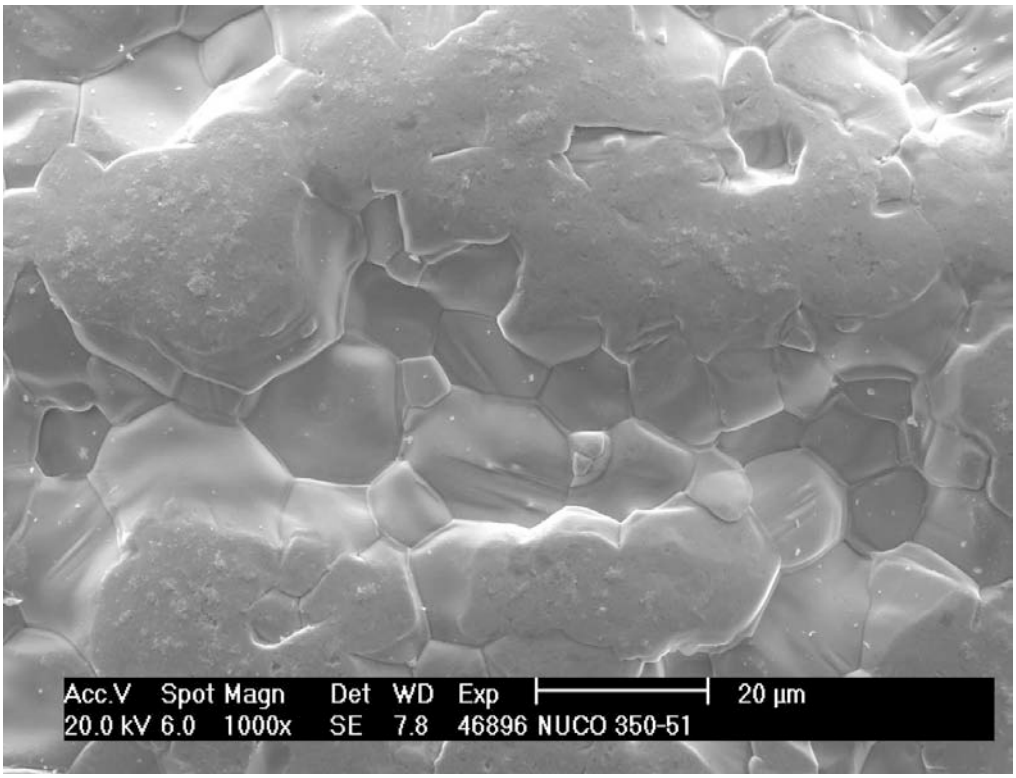

Figure 2-12: Lumpy NUCO kernel from 59344 batch.

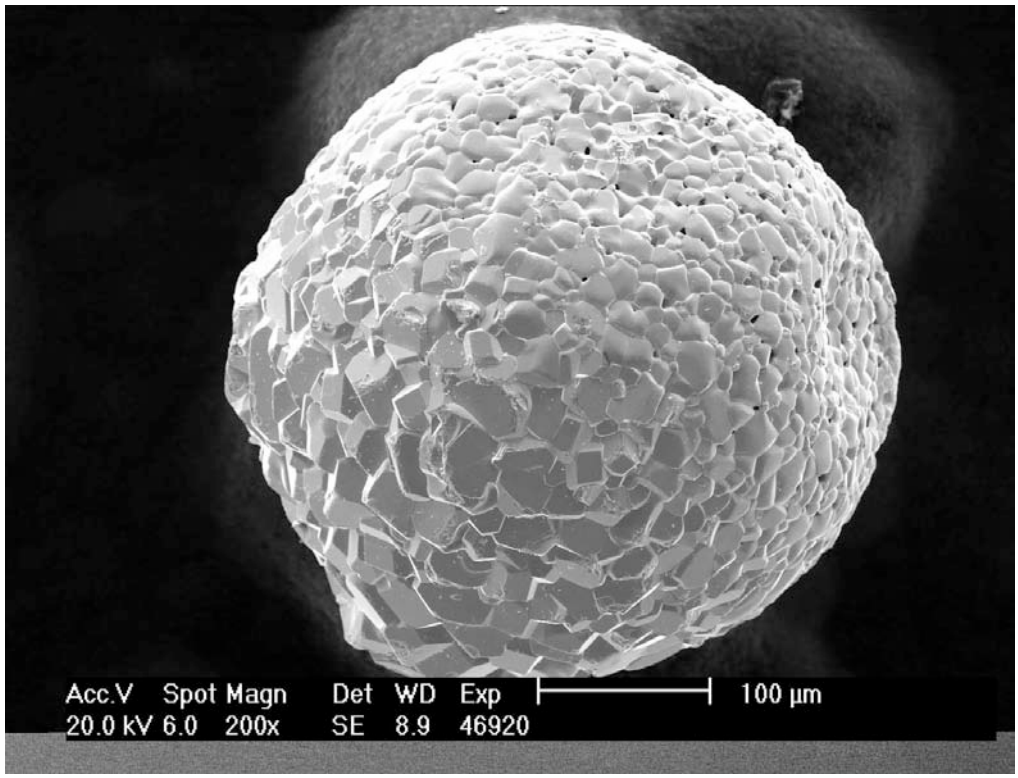

Figure 2-13: NUCO kernel from 59344 batch showing unusually large crystalline grains.

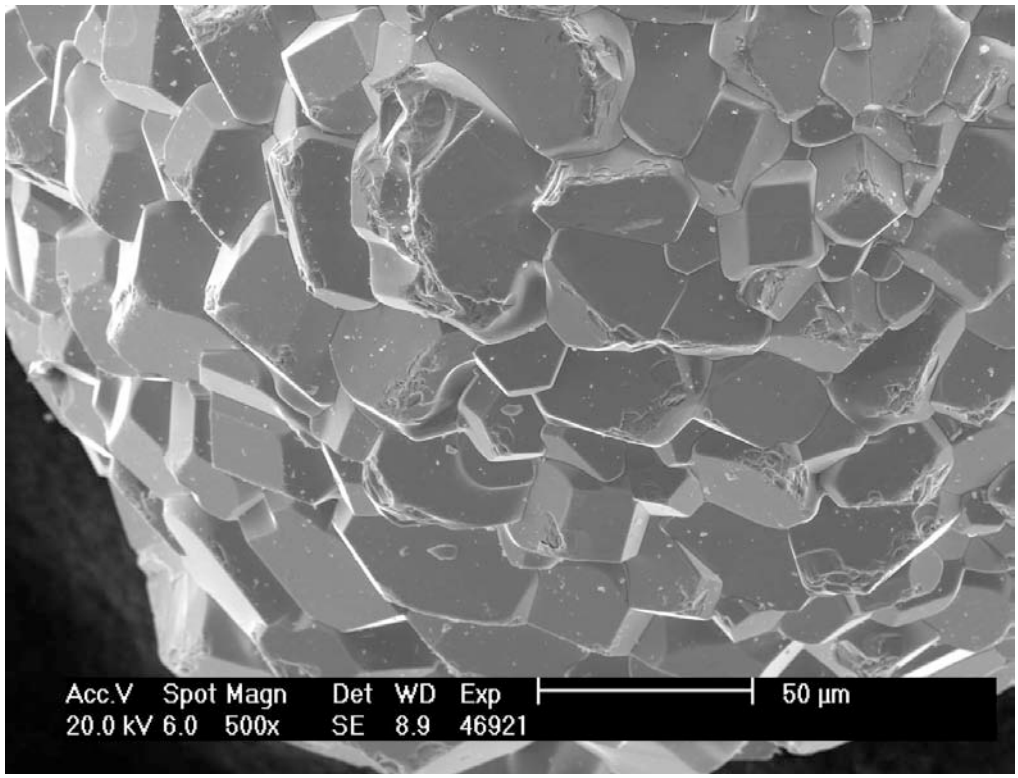

Figure 2-14: NUCO kernel from 59344 batch showing unusually large crystalline grains.

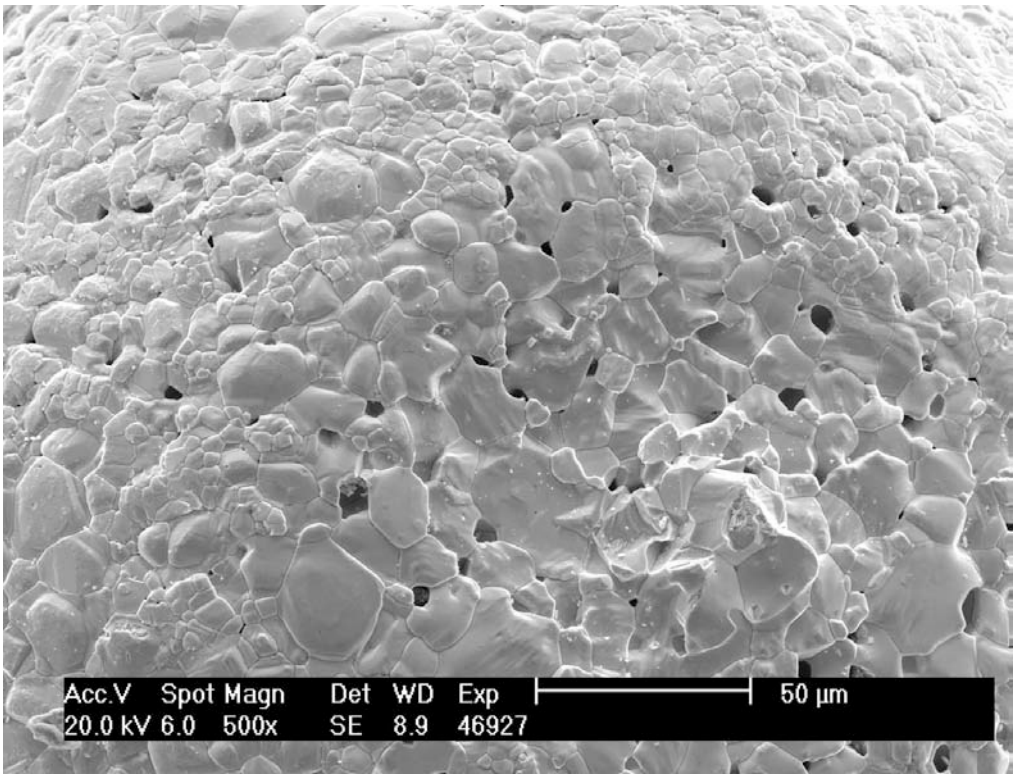

Figure 2-15: Back side of NUCO kernel in Figure 2-14.

3 SEM Analysis of Kernel Polished Cross-sections

J.D. Hunn and P.A. Menchhofer

Kernels were mounted in conductive epoxy and ground and polished to near the midplane. Figure 3-1 and Figure 3-2 show an example of a smooth and a lumpy kernel in cross section in normal scanning electron mode (tomographically sensitive). The lumpy kernels were typically much more porous than the smooth kernels, as can be seen for the pair of kernels in these images.

SEM imaging using backscattered electrons provides imaging contrast as a function of atomic number, density and channeling. Figure 3-3 shows a typical smooth NUCO kernel cross section. The brightest areas are carbide grains. Oxide containing grains have a lower density and appear gray in this image. The black spots are pores. The kernel in Figure 3-3 shows a mixture of carbide and oxide regions in the interior, surrounded by an oxide rich rind (the rind was often absent in the bumpy kernels). Energy dispersive x-ray spectroscopy (EDS) showed that the gray oxide regions actually contain a significant amount of carbon as well. However, the brighter carbide regions do not show appreciable oxygen content. Closer analysis shows additional microstructure in the carbide regions (Figure 3-4 and Figure 3-5). Bands could be seen which were apparently oriented with the grain direction. The relative size of the EDS peak for carbon indicated that the darker bands are probably the lower density dicarbide ($UC_{1.86}$) and the brighter areas are probably monocarbide (UC).

Figure 3-6 shows a kernel that did not exhibit the oxide depleted carbide phases that are usually seen in the interior of each kernel. The entire kernel showed a mixture of uranium, carbon, and oxygen in the EDS analysis. Figure 3-7 through Figure 3-9 show that this kernel was unusually porous. This higher porosity had the effect of making the interior chemistry similar to the rind chemistry in other kernels.

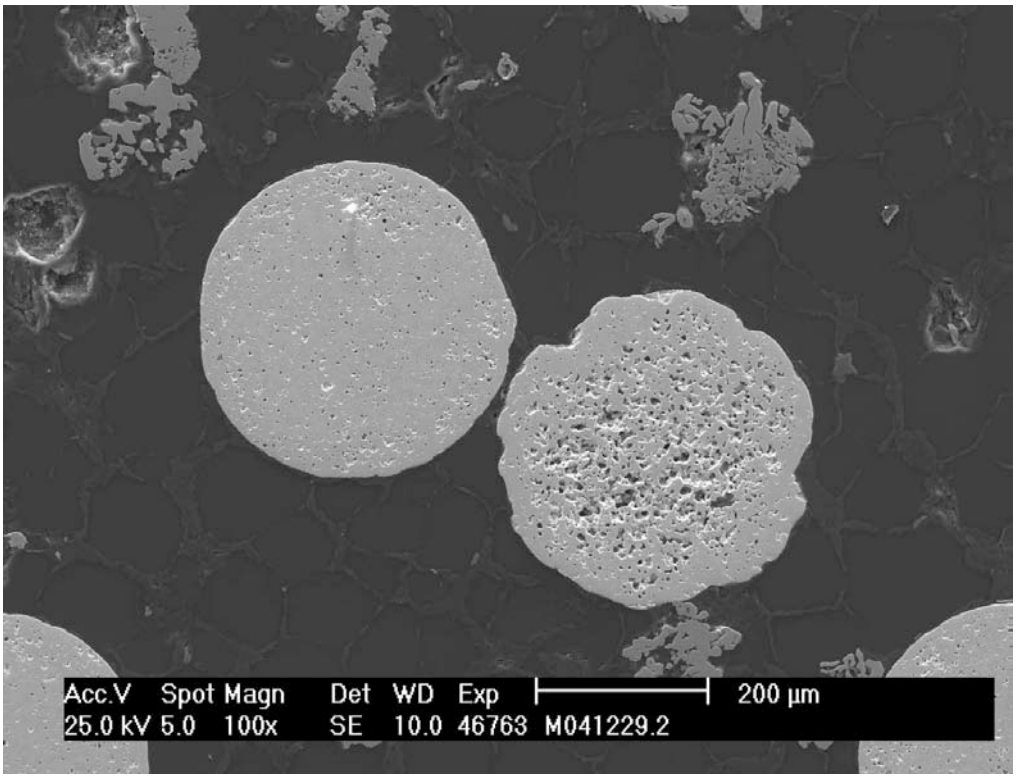

Figure 3-1: Cross section of smooth and lumpy kernel.

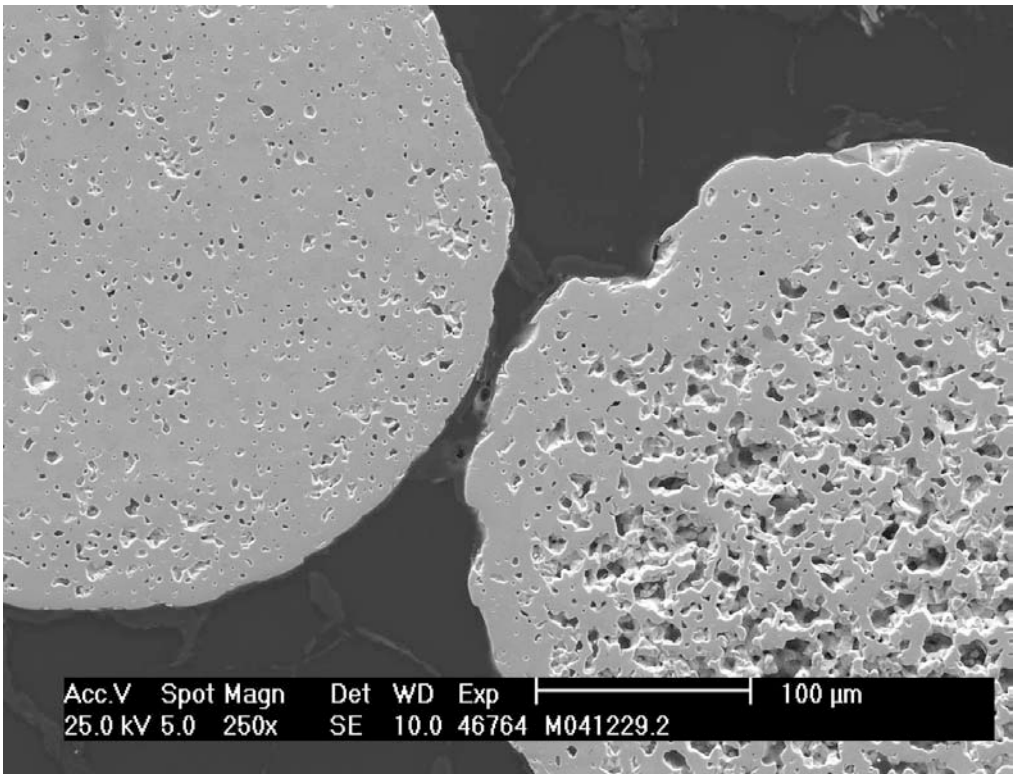

Figure 3-2: Cross section of smooth and lumpy kernel.

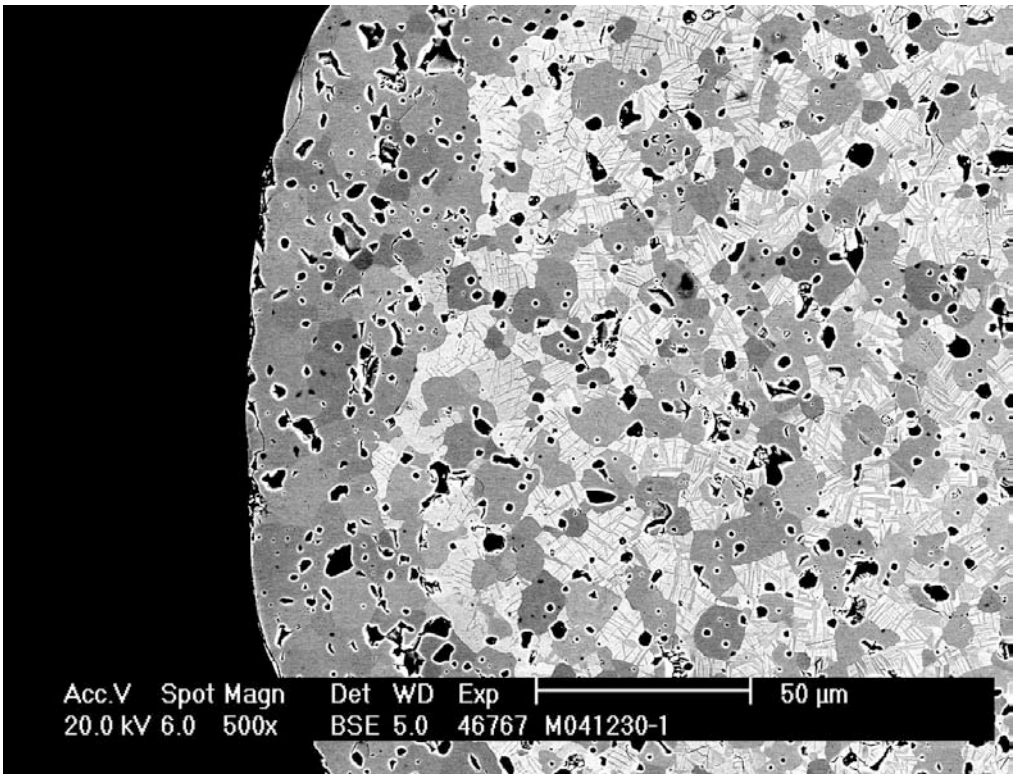

Figure 3-3: Smooth kernel cross section imaged with backscattered electrons.

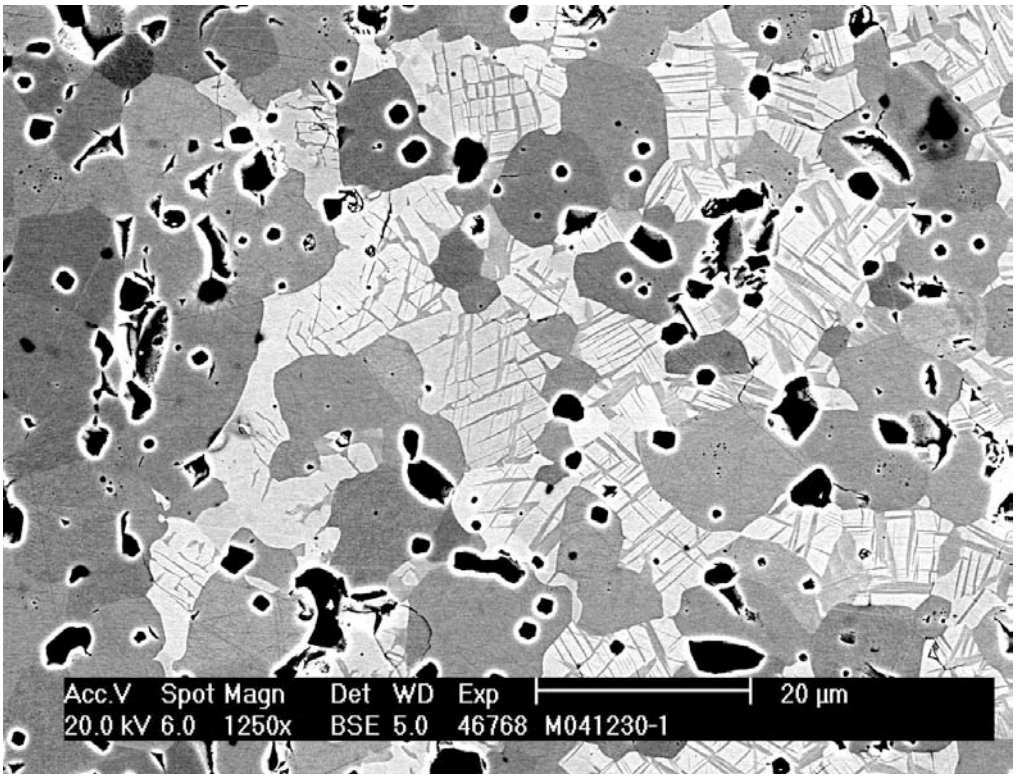

Figure 3-4: Smooth kernel cross section imaged with backscattered electrons.

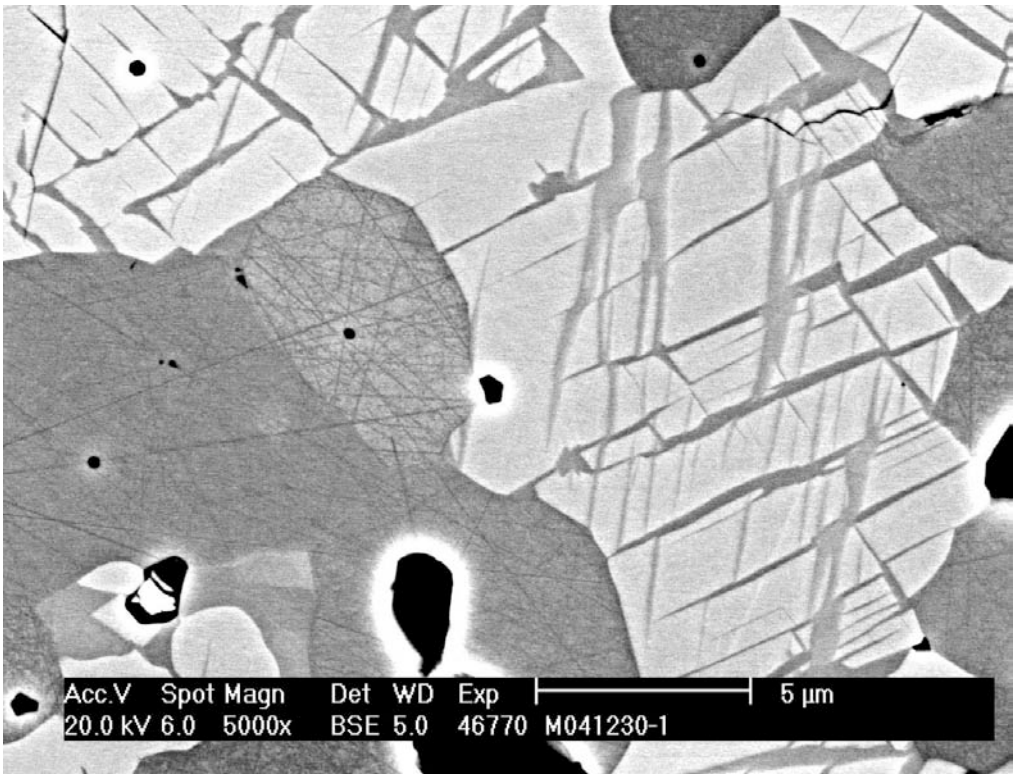

Figure 3-5: Smooth kernel cross section imaged with backscattered electrons.

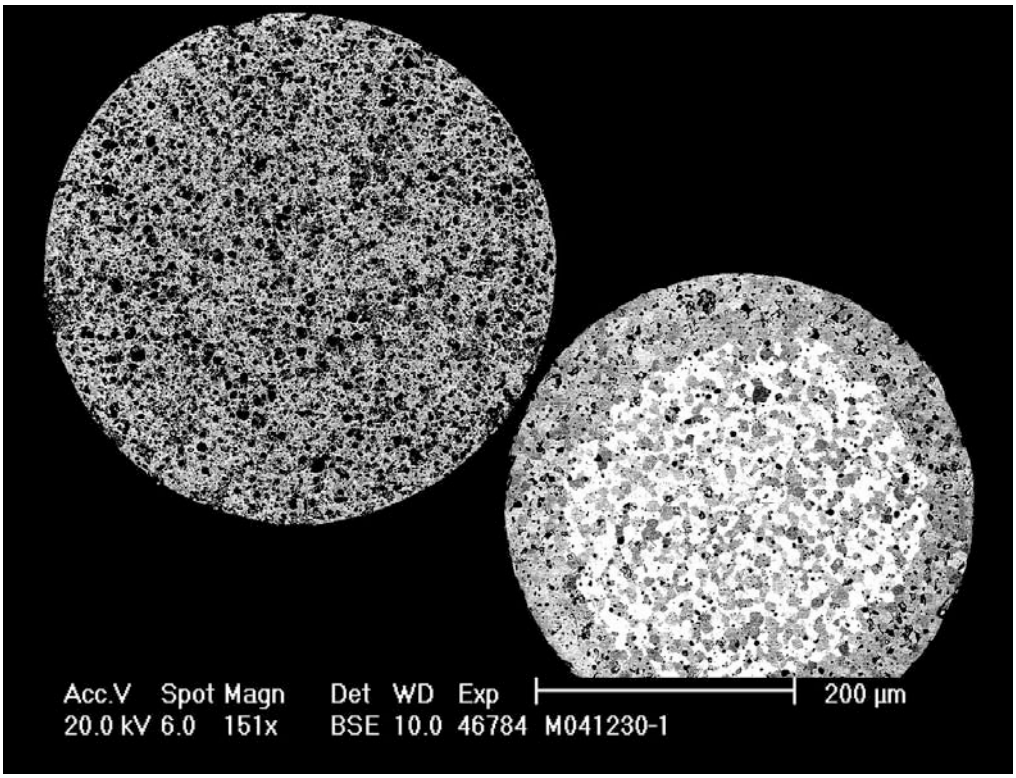

Figure 3-6: Kernel without carbide phases (upper left).

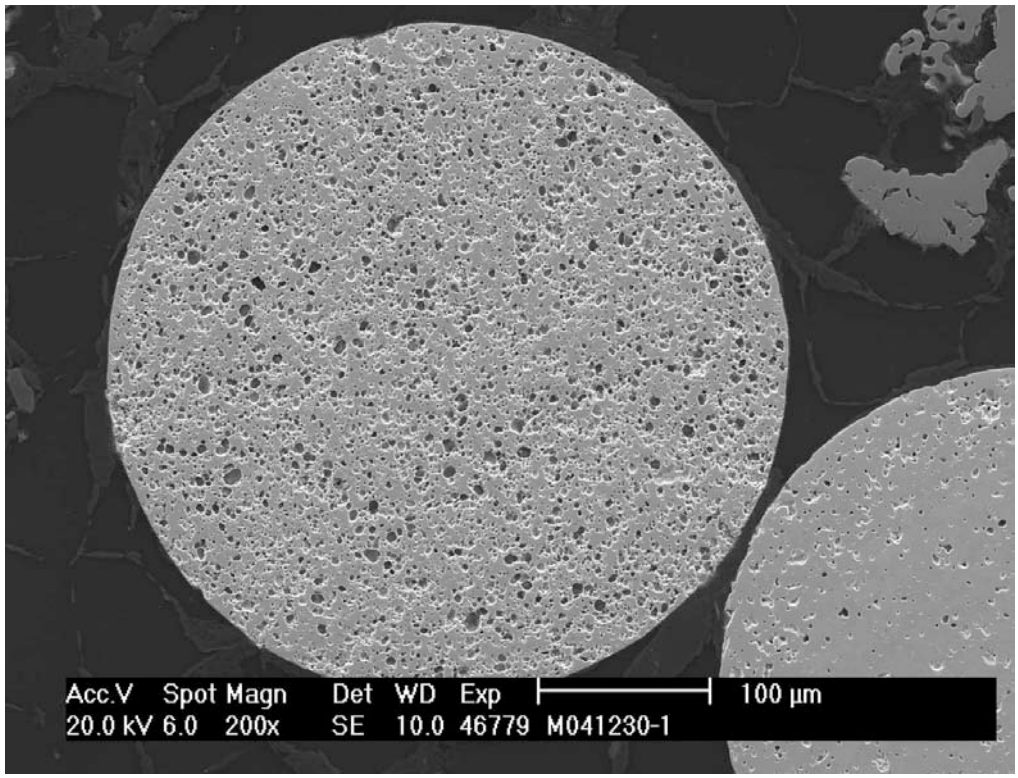

Figure 3-7: Kernel without carbide phases.

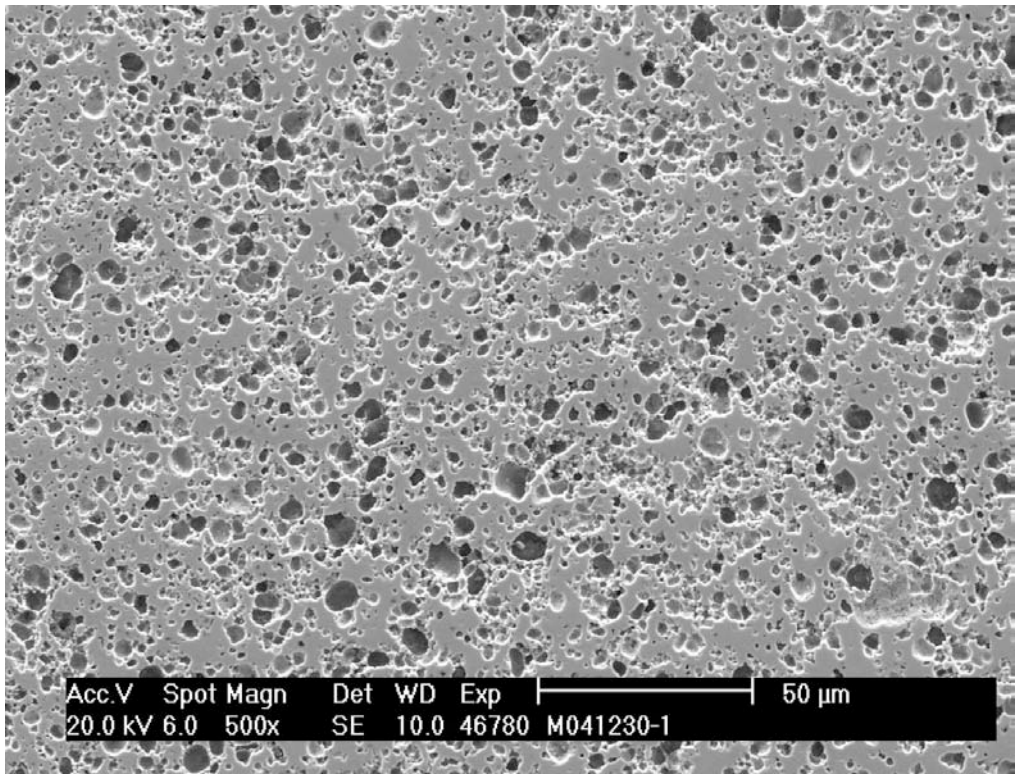

Figure 3-8: Kernel without carbide phases.

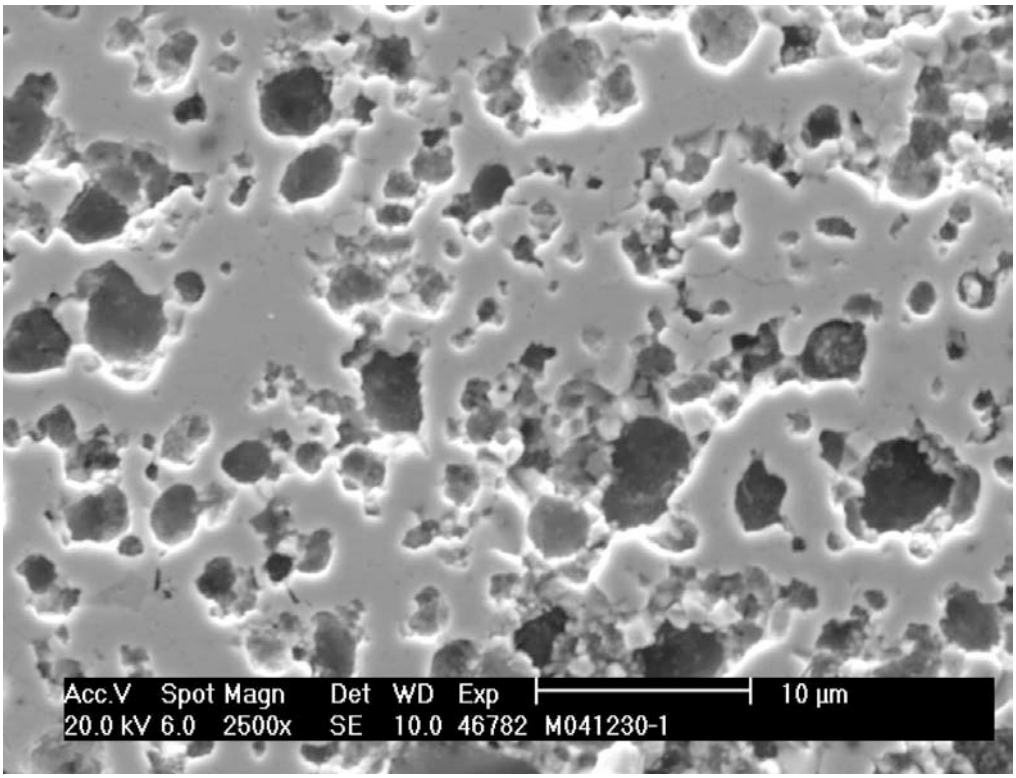

Figure 3-9: Kernel without carbide phases.

4 Analysis of Kernel Polished Cross Section After Coating

J.D. Hunn and P.A. Menchhofer

A TRISO coating was applied to a sample of kernels from batch 59344. Previous observations on coated kernels from the 69300 composite have shown that during the SiC deposition (1400-1500°C for ~2 hours) the kernels react with the carbon in the buffer layer to form a uranium carbide skin at the interface. These observations and an explanation of the effect can be found in Appendices A and B. Formation of a carbide skin was observed for the coated kernels from batch 59344 as well. Figure 4-1 shows an optical micrograph of one of these coated particles. The white ring between the kernel and the buffer is the carbide skin that formed during coating. Notice that this ring is broken away from the rest of the kernel.

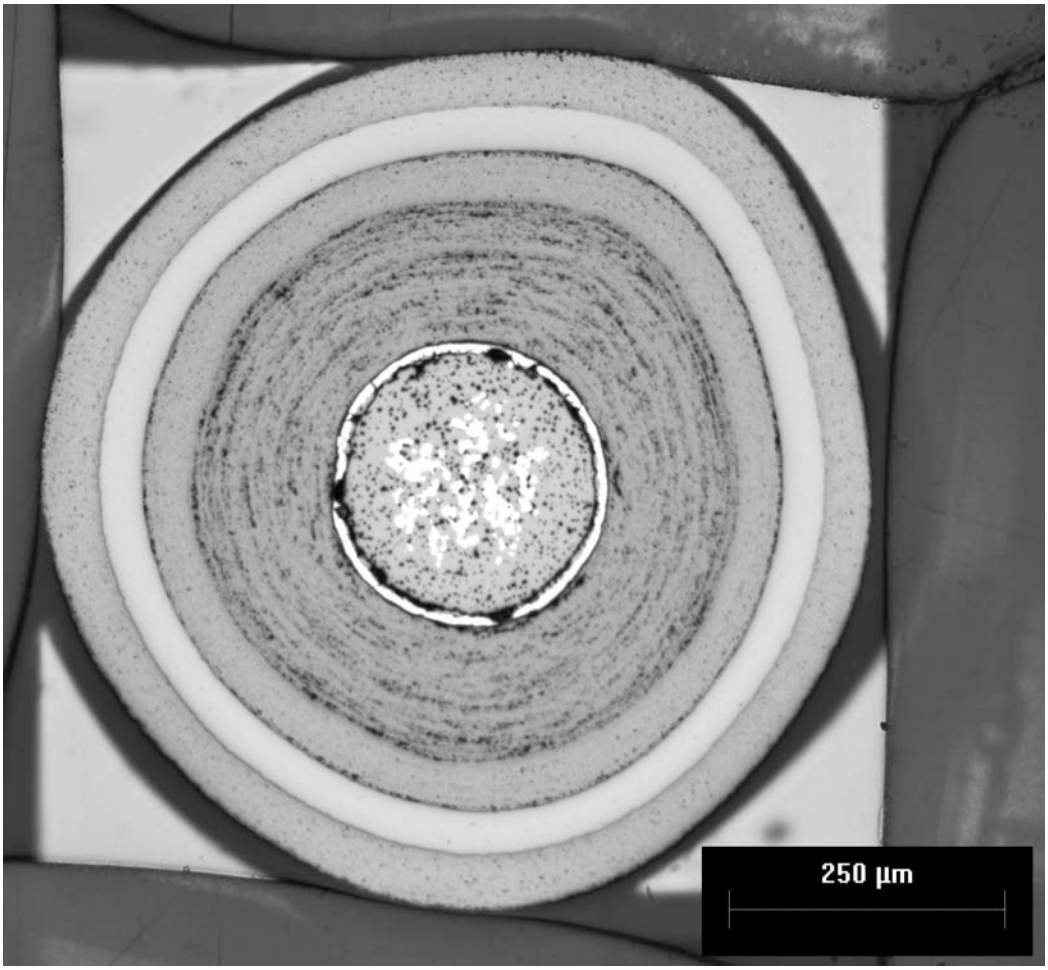

Figure 4-1: Optical micrograph of cross section of TRISO coated NUCO kernel.

Additional SEM analysis was performed on the NUCO kernels after coating. Figure 4-2 through Figure 4-4 show a smooth kernel after coating. These figures can be compared to Figure 3-3 through Figure 3-5 for a similar kernel before coating. Figure 4-2 shows portions of the broken carbide layer which has formed outside of the oxycarbide rind. A comparison between Figure 4-4 and Figure 3-5 shows that the microstructure of the carbide grains in the interior of the kernel has also changed. The previously observed two phase banding is gone and some residual lines are all that remain. EDS indicates that there is now just one carbide phase in these grains with a similar relative carbon content to the darker bands observed in Figure 3-5 (probably dicarbide). The conversion of monocarbide to dicarbide occurring in the interior of the kernel with the extra uranium moving to the kernel surface to react with the carbon there is in agreement with the discussion in Appendix B.

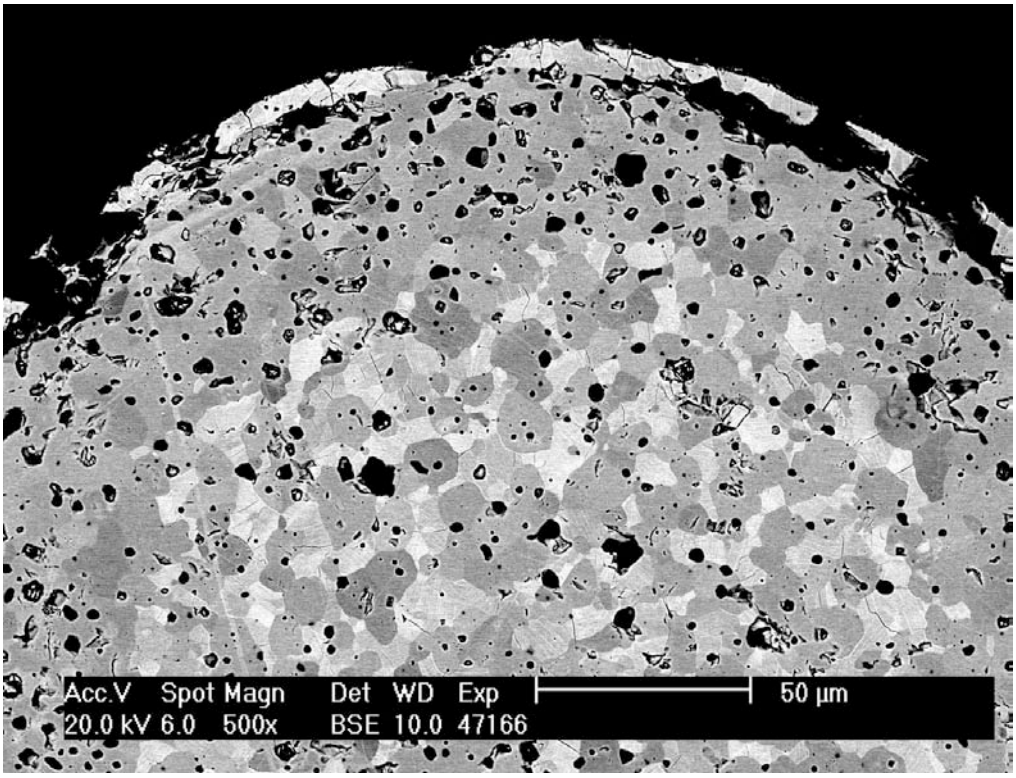

Figure 4-2: NUCO kernel from batch 59344 after TRISO coating.

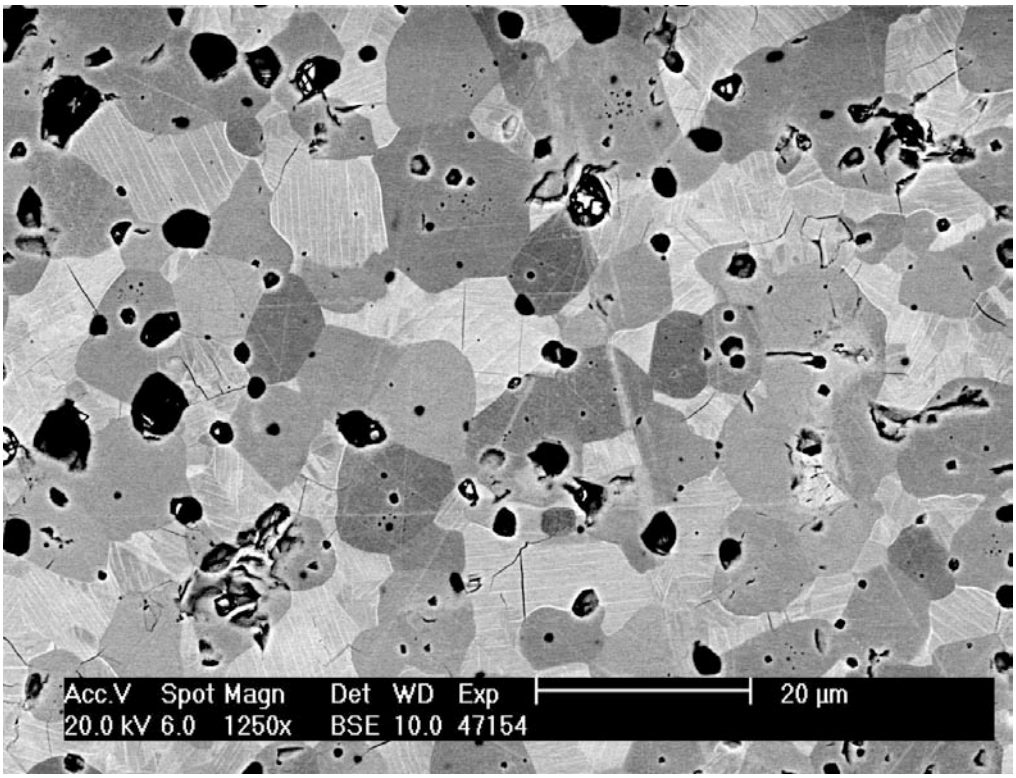

Figure 4-3: NUCO kernel from batch 59344 after TRISO coating.

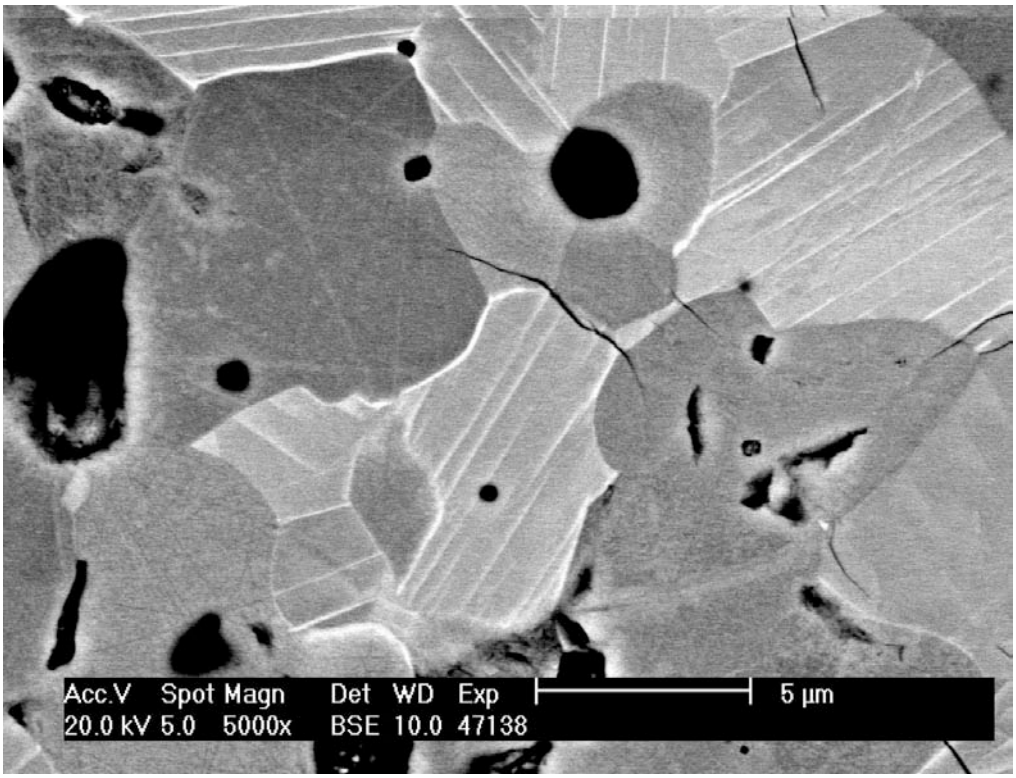

Figure 4-4: NUCO kernel from batch 59344 after TRISO coating.

5 Appendix A - Uranium carbide skin formation at kernel/buffer interface

John D. Hunn
Oak Ridge National Laboratory
November 30, 2004

This appendix summarizes observation made concerning the formation of a carbide skin on the surface of NUCO kernels from the 69300 composite after coating.

After coating we observed a white ring forming around the 350 μm NUCO kernels. SEM/EDS showed this ring to be uranium carbide. The carbide skin formed on both the smooth kernels (denoted as type 1 in ORNL/CF-04/07 "Results from ORNL Characterization of Nominal 350 μm NUCO Kernels from the BWXT 69300 composite") and on the bumpy kernels (denoted as type 3).

Type 1 kernels typically had an oxide rind, type 3 kernels sometimes had a rind and sometimes did not. Figure 5-1 and Figure 5-2 show uncoated 350 μm NUCO kernels. After applying the TRISO coating, a carbide skin was observed to have formed. Figure 5-3 through Figure 5-5 show examples. This skin did not form when coating UO_2 kernels (Figure 5-6).

In order to further understand this phenomenon, 350 NUCO was coated with only buffer and IPyC. Figure 5-7 and Figure 5-8 show that only a very thin skin, if any, could be observed on these particles.

The buffer/IPyC coated particles were annealed for 2 hours at 1400°C to simulate the heat treatment that occurs during SiC deposition. After annealing, a thick carbide skin had formed (Figure 5-9 through Figure 5-11). This skin is similar in thickness to that observed after TRISO coating. Heat treatment at higher temperature or longer periods did not change the thickness of the carbide skin, indicating that the reaction has gone to completion after 2 hours at 1400°C.

The conclusion is that the carbide skin is formed due to a reaction with the buffer layer rather than a reaction with the acetylene during buffer deposition. During buffer and IPyC deposition, the kernel buffer interface was at 1250°C for less than 30 minutes. Apparently at this temperature the carbide formation is slower. When the particles are heated to 1400°C for SiC deposition, the carbide formation apparently accelerates.

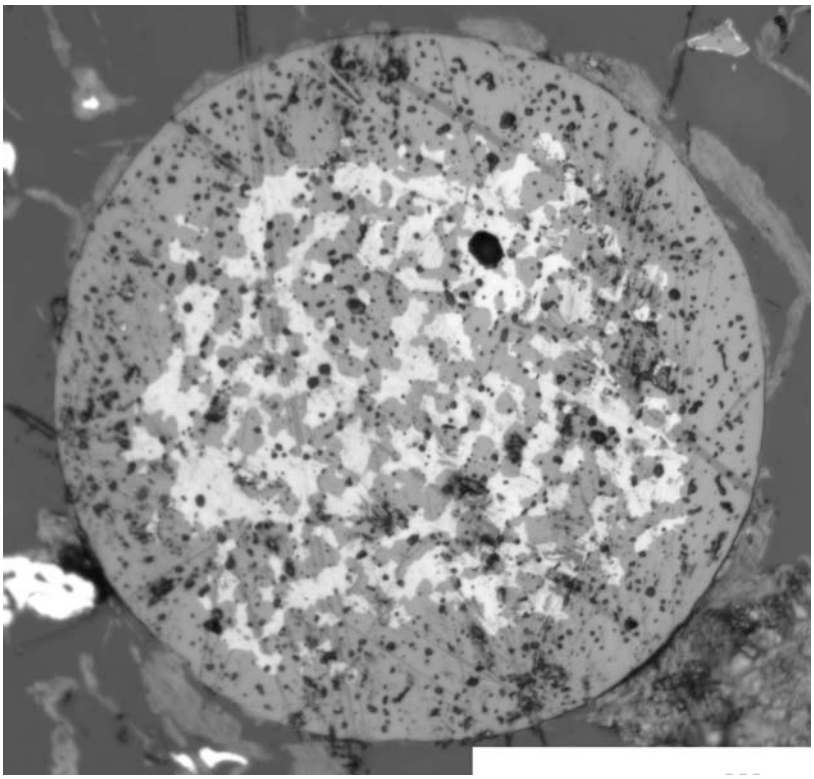

Figure 5-1: Type 1 350 μm NUCO kernel. Brightest regions are uranium carbide, grayer regions are uranium oxide (with possibly some carbon present).

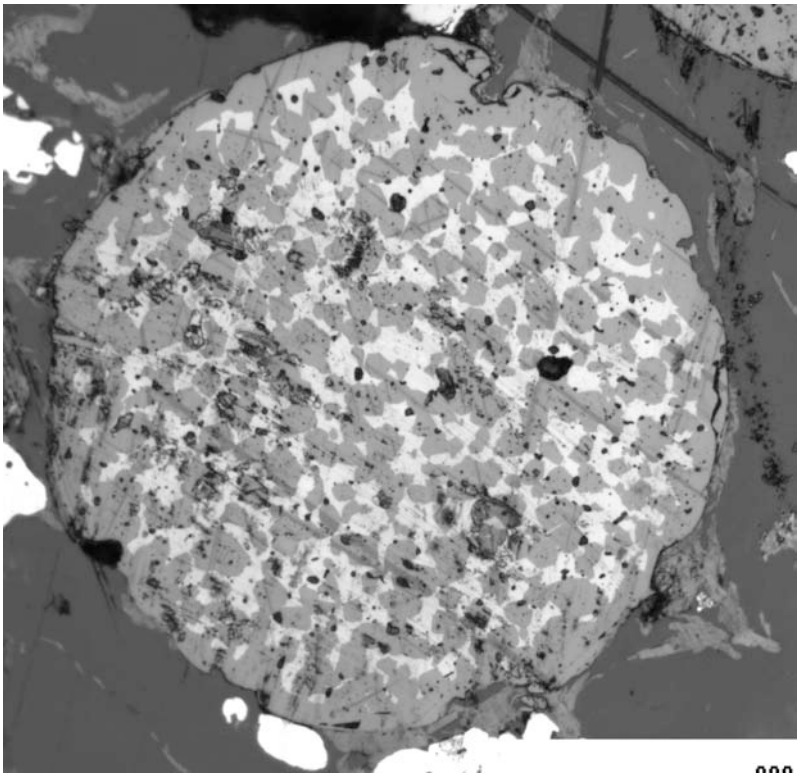

Figure 5-2: Type 3 350 μm NUCO kernel.

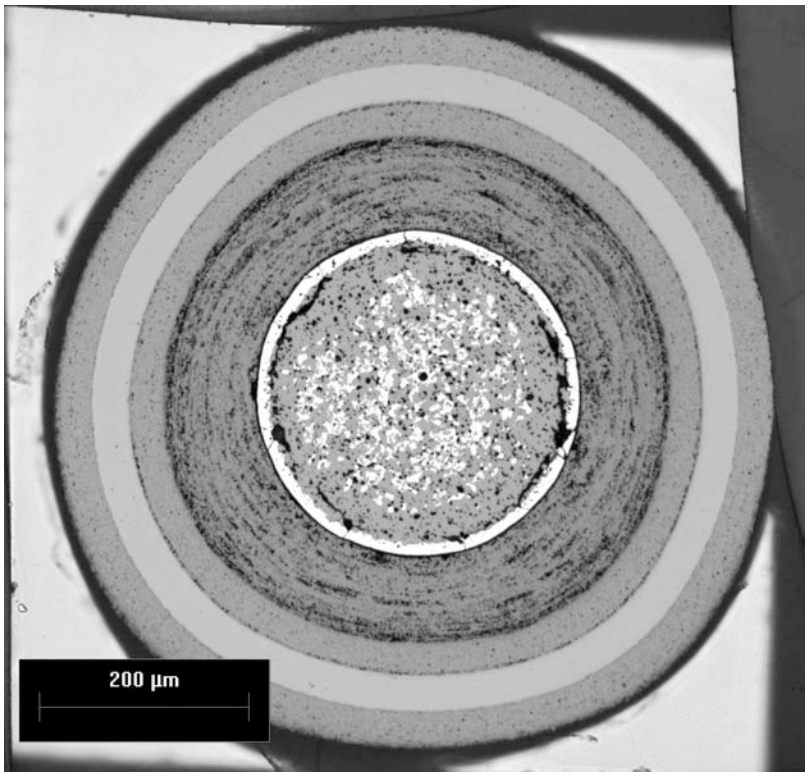

Figure 5-3: TRISO coated type 1 kernel. A thick carbide skin has formed.

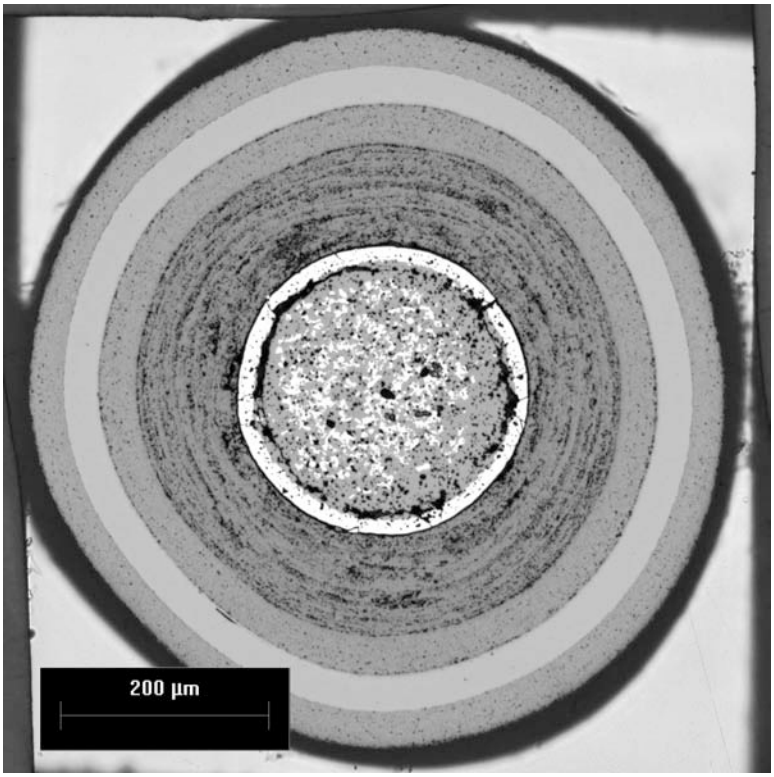

Figure 5-4: Another TRISO coated type 1 kernel.

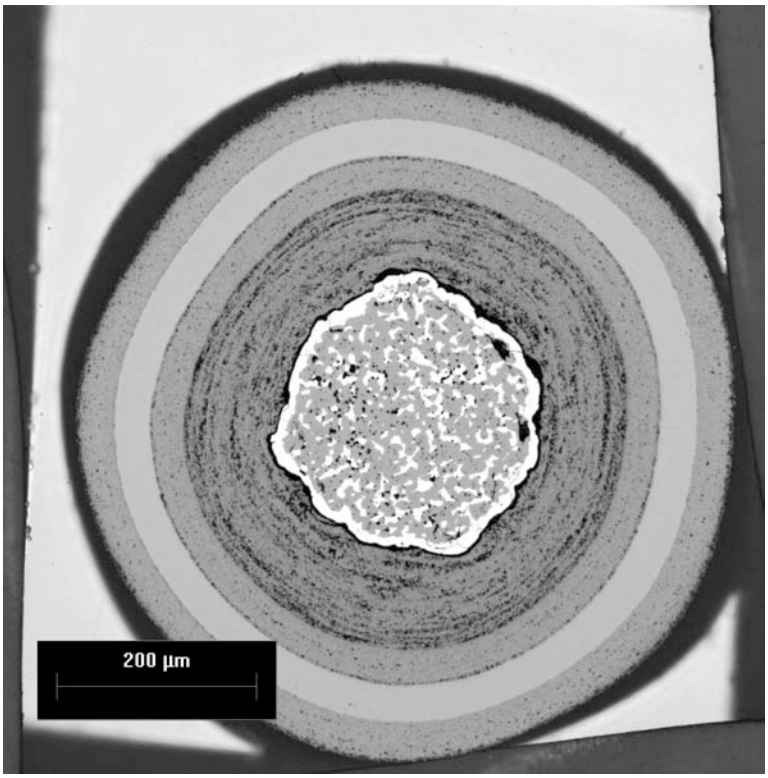

Figure 5-5: TRISO coated type 3 kernel. A similar carbide skin has formed. This kernel did not have an oxide rind.

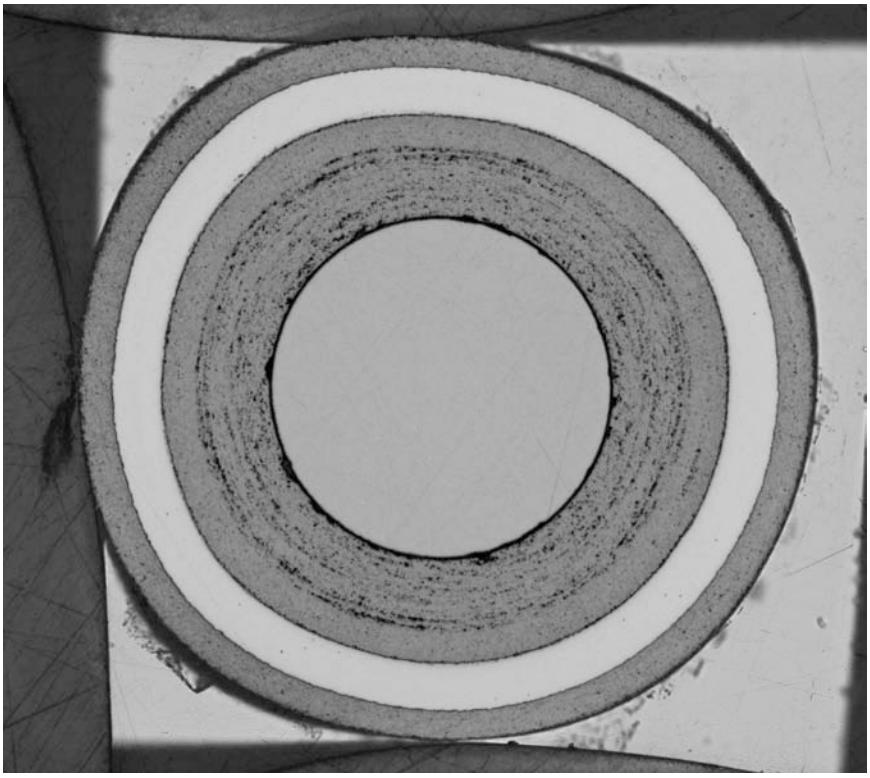

Figure 5-6: The carbide skin is not observed on coated UO_2 kernels such as seen here.

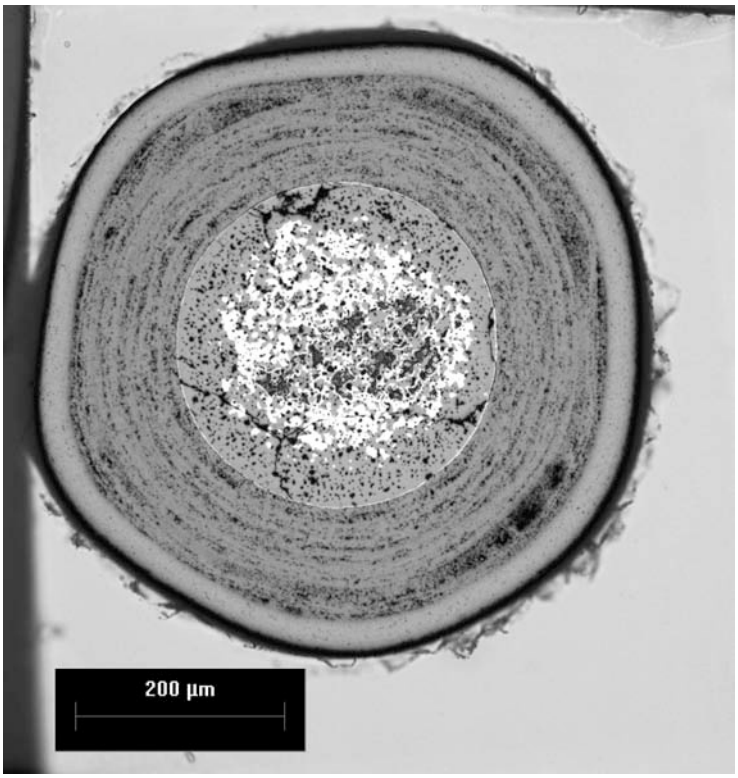

Figure 5-7: Only a very thin carbide skin formed during buffer and IPyC coating.

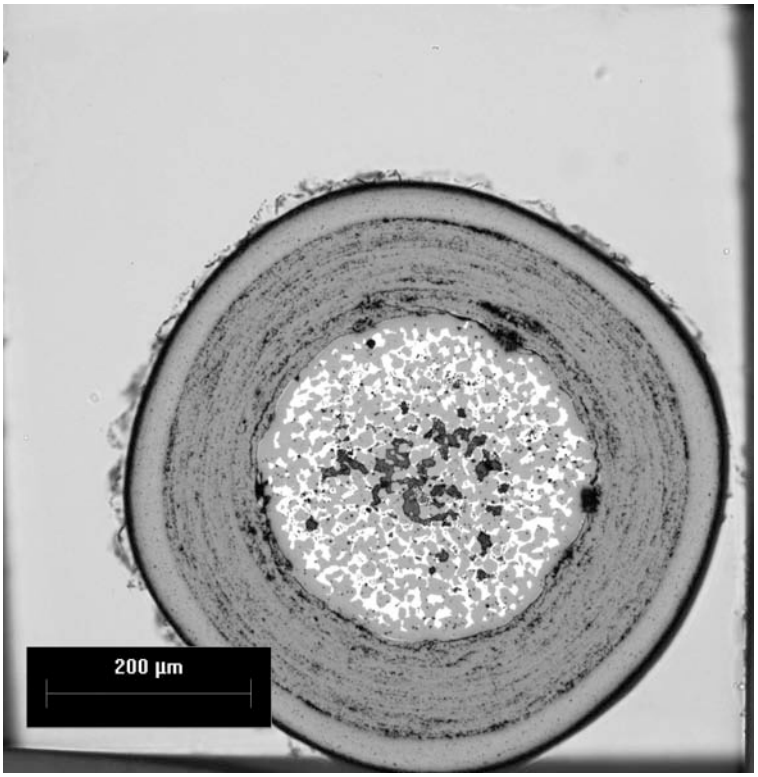

Figure 5-8: Only a very thin carbide skin formed during buffer and IPyC coating.

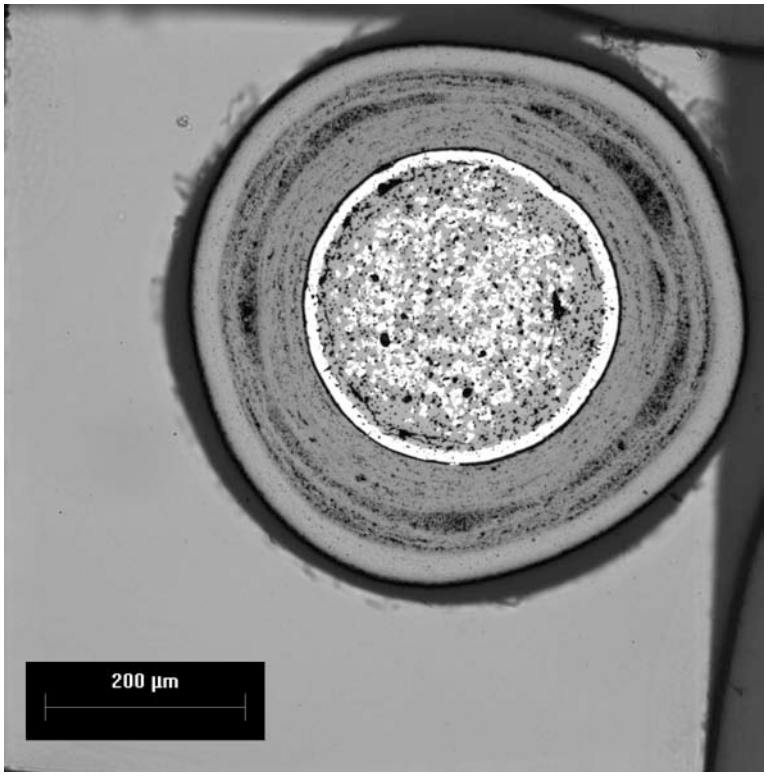

Figure 5-9: A thick carbide skin formed during heat treatment at 1400°C for 2 hours.

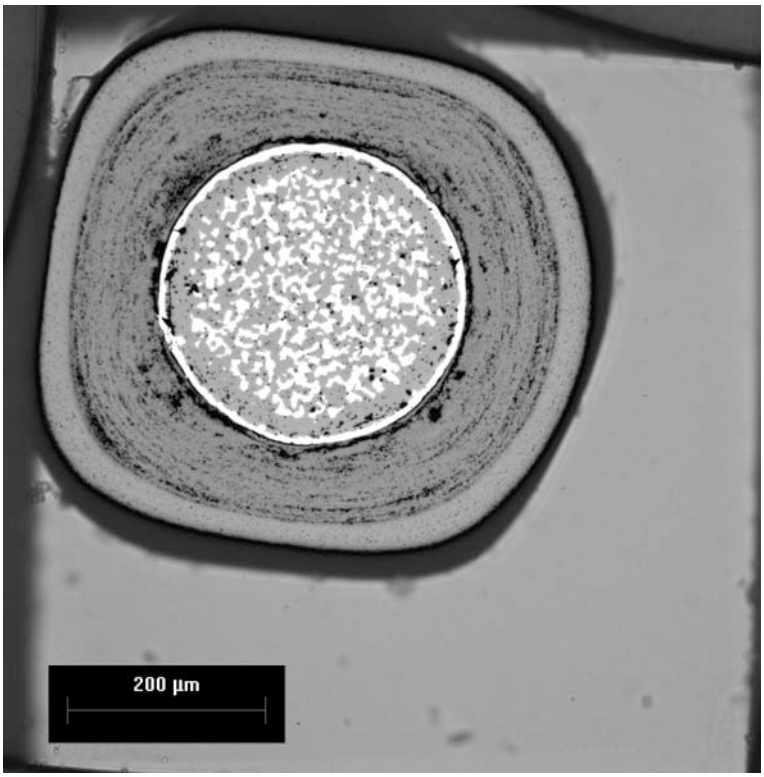

Figure 5-10: A thick carbide skin formed during heat treatment at 1400°C for 2 hours.

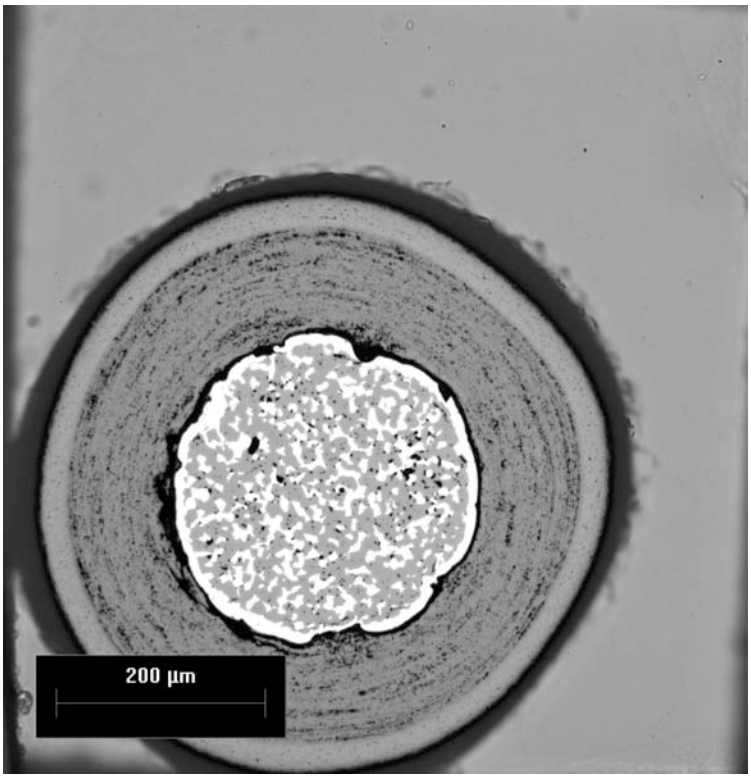

Figure 5-11: A thick carbide skin formed during heat treatment at 1400°C for 2 hours.

6 Appendix B - Analysis of Carbide Redistribution in Coated NUCO Kernels

Terrence B. Lindemer
Harbach Engineering and Solutions, Inc.
Nov. 21, 2004

Summary: Quantitative ceramography combined with mass-balance calculations and correction of the plane-of-polish dimensional measurements to those at the kernel midplane reveal that the carbide outer layer seen on coated NUCO oxide-carbide kernels is consistent with redistribution of the original UC content during TRISO coating. No additional carbide is formed during this redistribution and carbothermic conversion plays no role. This redistribution has also been seen in irradiated German fuel and is not believed to be an important effect. Formation of this layer could apparently be prevented only by converting the UC to dicarbide during kernel manufacture.

Introduction: During the week of Nov. 15 John Hunn provided a written summary that included photomicrographs of Type 1 and Type 3 NUCO, 350-micron-diameter, oxide-carbide kernels before coating and after different stages of coating and corresponding times at temperature (see Appendix A). An outer layer of carbide was observed on the kernel in the coated particles only after heating at 1400 ºC for 2 hours. These photomicrographs were analyzed by quantitative ceramography and the results were used to explain the origin of and mechanism for the formation of the outer carbide layer.

Kernel Chemistry: The NUCO material is a mixture of kernels from several conversion runs produced by BWXT and identified by Run 69300. The O/U and C/U values for the batch mixture are 1.299 and 0.400 and these values lead to 0.649 mol fraction urania (UO_2), 0.293 mol fraction UC and 0.058 mol fraction $UC_{1.86}$. In the as-manufactured kernel this is equivalent to 0.237 and 0.057 volume fraction, respectively, for a total of 0.294. It is assumed in this analysis, as will be described later, that heating at 1400 ºC during TRISO coating results in conversion of the UC to $UC_{1.86}$ and the total volume fraction of the latter would be 0.327 of the entire kernel.

Quantitative Ceramography: Quantitative ceramography was performed on images of both kernel types before coating and after the 1400 ºC heat treatment. The uncoated Type 1 kernel contained the carbide phase in the core of the kernel, while the Type 3 kernel had a nearly uniform distribution of carbide across the entire kernel. The images of the kernels were examined quantitatively at 200% on the computer monitor. Similarly, the TRISO-coated Type 1 and 3 kernels were examined at 500%. For example, for the Type 1 kernel the volume fraction of carbide in the core was measured by placing a centimeter ruler across six locations in the core (only) and counting the intersections of the centimeter marks with the carbide phase. The number of intersections divided by the total number of available centimeter marks on the ruler for the six locations across the core is the volume fraction of carbide; this measurement is called the point-count method.

The type 1 kernel will be analyzed first. The core of the uncoated kernel had 46 carbide intersections out of a total of 99 possible and thus the volume fraction of carbide was 0.469. This

is typical of a kernel with the wide carbide-free outer oxide rind; the overall 0.237 plus 0.057 or 0.294 volume fraction carbide calculated from the chemical analysis is concentrated in the core. The kernel in the TRISO-coated particle was analyzed next and permits a quantitative mass balance of carbide content. The core of this kernel had 31 carbide intersections out of a possible 107 to give 0.290 volume fraction carbide. It is immediately obvious from comparison with the uncoated kernel that the carbide concentration in the core has decreased. To continue, the thickness of the carbide outer layer was measured at several locations and the average thickness was determined to be 13.8 microns. Similarly, on the plane of polish the diameter of the kernel was 277 microns and the carbide-containing core diameter was 194 microns. At this point there is sufficient information to calculate a true carbide volume balance, but dimensions at the kernel mid-plane are needed. Thus, plane-of-polish measurements were corrected to true dimensions using the Pythagorean relationship and the 175-micron radius of the kernel. The height of the plane of polish above the equator is calculated to be $(175^2 - [277/2]^2)^{0.5}$ or 107 microns. The true radius of the carbide-containing core was calculated similarly to be144 microns and the relative volume of the core is $(144/175)^3$ or 0.557 of the entire kernel. The inner radius of the carbide outer layer is $(107^2 + [277/2 - 13.8]^2)^{0.5}$ or 164.3 microns, the true thickness is 10.7 microns, and it follows that the outer carbide layer is 1- $([175\text{-}10.7]/175)^3$ or 0.172 of the total volume of the kernel. The volume fraction of $UC_{1.86}$ in the entire kernel is that in the outer layer and in the core and is 0.172 + 0.29(0.557) or 0.334. This compares remarkably well with the 0.327 calculated from the chemical analysis and assuming that all the UC was converted to $UC_{1.86}$.

The Type 3 kernel was analyzed also. The volume fraction of carbide in the uncoated kernel was determined by point count and was 44/134 or 0.328. This value is slightly higher than the 0.294 calculated from the chemical analysis, but Type 3 kernels have a slight carbide-free outer layer and taking this into account would bring the two into agreement. In the TRISO-coated particle the volume fraction carbide is 29/113 or 0.26. Again, the carbide content is lower than in the uncoated kernel. Four measurements of the diameter on the plane of polish averaged 253 microns, and five measurements of the thickness of the carbide layer averaged 8.0 microns. Again assuming that the kernel diameter is 350 microns, the height of the plane-of-polish above the equator is 121 microns and the true diameter of the inner surface of the carbide layer is 169 microns, which gives a true carbide thickness of 6 microns and this layer occupies 0.10 of the volume of the kernel. The relative volume of the carbide-containing inner region is thus 0.9. The volume fraction of $UC_{1.86}$ in the entire kernel is calculated to be 0.10 + 0.9(0.26) or 0.334, which is identical to that in the Type 1 kernel and again compares well with the 0.327 calculated from the chemical analysis.

Proposed Mechanism for Carbide Redistribution: It is clear from the above that the carbide redistributes during the 1400 ºC heat treatment, but the before-and-after carbide content satisfies the carbon balance almost exactly. Also, since TRISO-coating of urania does not result in carbide formation and since it is generally recognized that the IPyC is impervious to CO, it is also clear that the carbide layer cannot have been formed by carbothermic conversion. Proposed here as a mechanism for this carbide redistribution is a three-step process,

Step 1 $UC = (1/1.86)\ UC_{1.86} + (1 - 1/1.86)\ [U]_{oxide}$ in the interior of the kernel

Step 2 Diffusion of $[U]_{oxide}$ through the urania phase to the surface

Step 3 $[U]_{oxide} + 1.86\ C = UC_{1.86}$ at the surface

in which $[U]_{oxide}$ is uranium dissolved in the urania. The first step results from the closed thermodynamic system seeing a carbon activity of unity, but does not require diffusion of carbon from the buffer layer. If the latter took place, then the monocarbide would simply convert to dicarbide in place and no outer layer would form.

The activity gradients seem proper for this process. In the interior of the kernel the carbon activity is defined by the equilibrium between the two carbides and is less than unity (roughly, ~0.8, as derived from Fig. 6 of ref. 1), while the activity is at unity at the surface where the buffer carbon is located. Since the oxide-carbide equilibrium defines the oxygen potential as a constant in the coated particle and since the carbon activity is lower in the kernel, the uranium activity must be higher in the interior than at the surface of the kernel. Thus, uranium diffuses down its activity gradient to the surface.

It appears from the above that the redistribution of the UC component would be prevented if kernel manufacture provided $UC_{1.86}$ and urania as the two phases. However, this redistribution does not appear to be deleterious, as is discussed below.

Similar German results: In November David Petti of INEEL asked Heinz Nabielek, formerly a research staff member on the gas-cooled-reactor project at KFA Jülich, for any information on UCO irradiation and ref. 2 was provided electronically. This report briefly describes the irradiation conditions for TRISO-coated, 300-micron-dia., oxide-carbide kernels irradiated in FRJ2-P24 to 18.6-22.2% FIMA and provides ceramography of as-coated and irradiated particles. (Jim Kendall also provided ref. 3, which is the extensive analysis of the irradiation, but the report contains no ceramography of individual particles.) The chemical analysis of the as-manufactured kernel was 91.56, 1.88 and 6.25 wt.% U, C, and oxygen, respectively. This composition is equivalent to O/U = 1.016 and C/U = 0.403 and a two-phase kernel made up of 0.419 mols of UO_2 and 0.581 mols of $UC_{0.694}O_{0.306}$. The monooxycarbide composition is consistent with that expected from the usual high-temperature carbothermic conversion and sintering, particularly if it were performed in either argon or vacuum, i.e., without the Ar-60%CO atmosphere used in the BWXT process, as can be deduced from ref. 1. The density of the kernel was given as 11.18 g/cm^3 and with these two phases the density of the kernel may have been about 90% of theoretical; obvious kernel porosity is evident in the ceramography. Figures 2 and 3 of ref. 2 show ceramography of unirradiated TRISO-coated particles that are essentially identical in appearance with ORNL TRISO-coated Type 1 and 3 kernels and demonstrate that the present ORNL observations are consistent with the German results. Therefore, after TRISO coating, the $UC_{0.694}O_{0.306}$ of the German fuel probably redistributed to give a total of 0.419 + 0.306/2 or 0.572 mols of UO_2 and 0.581 – 0.306/2 or 0.428 mols of $UC_{1.86}$.

Ceramography of irradiated material in ref. 2 reveals kernel porosity that was different in appearance from that in the original kernel, some localized penetration of the kernel across the buffer layer and up to the IPyC, but no generalized kernel migration and no apparent attack of the SiC layer.

Consequences of carbide redistribution: According to ref. 4 and 5, the effect of this carbide outer layer on the kernel performance was briefly discussed during the generation of the NRC PIRT report (ref. 6) and was not considered to be a very important factor in overall performance because there is no published data indicating that it is a significant failure mechanism for TRISO fuel. The implications of the UO_2 - C reaction were not considered because this kernel rind formation was a manufacturing issue beyond the scope of the report.

References

1. T. M. Besmann, "Thermodynamic Measurements and Modeling of $<UC_{1-x}O_x>$," J. Am. Ceramic Soc. 66 (1983) 353-358.

2. Ch. Bauer and H. Klöcker, "Elektrolytische Desintegration an 3 Compacts aus dem Experiment FRJ2-P24," KFA Jülich internal report IRW-IN-8/83, (1983) 15 pp.

3. G. Borchardt, B. Hürttien and G. Pott, "Experiment FRJ2-P24 Bestrahlungsbericht," KFA Jülich internal report KFA-ZBB-IB-19/82 (Aug. 23, 1982) 40 pp.

4. D. A. Petti, private communication by email from INEEL to Gary Bell of ORNL dated 11/12/2004.

5. R.A. Morris, private communication.

6. "TRISO-Coated Particle Fuel Phenomenon Identification and Ranking Tables (PIRTs) for Fission Product Transport Due to Manufacturing, Operations, and Accidents," NUREG/CR-6844, Vol. 1, July 2004.

ADVANCED GAS REACTOR PROGRAM
OAK RIDGE NATIONAL LABORATORY

ORNL DOCUMENT CLEARANCE / REGISTRATION FORM

PERSON PREPARING FORM:	PHONE NO.:	DATE SUBMITTED:
Jan Z. Palmer	576-7054	January 26, 2005
DOCUMENT NO.:	**SPONSOR:**	
ORNL/CF-05/02	DOE-NE / Dr. Madeline Feltus	

TITLE:

Results from ORNL Characterization of Nominal 350 μm NUCO Kernels from the BWXT 59344 Batch

AUTHOR(s):

John Hunn, Andrew K. Kercher, and Paul A. Menchhofer

SIGNATURES:

AUTHOR:

John Hunn — 2-2-05

Name: John D. Hunn — Date

TECHNICAL REVIEWER:

O. M. Stansfield — 2/3/05

Name: O. M. Stansfield — Date

APPROVER:

Gary L. Bell — 3 Feb 05

Name: Gary L. Bell — Date